NeuroImage 299 (2024) 120844

Contents lists available at ScienceDirect

NeuroImage

journal homepage: www.elsevier.com/locate/ynimg

Plastic reorganization of the topological asymmetry of hemispheric white matter networks induced by congenital visual experience deprivation

Saiyi Jiao [a], Ke Wang [a,b], Yudan Luo [a,c], Jiahong Zeng [a], Zaizhu Han [a,*]

[a] National Key Laboratory of Cognitive Neuroscience and Learning & IDG/McGovern Institute for Brain Research, Beijing Normal University, Beijing 100875, China
[b] School of System Science, Beijing Normal University, Beijing 100875, China
[c] Department of Psychology and Art Education, Chengdu Education Research Institute, Chengdu 610036, China

ARTICLE INFO

Keywords:
Asymmetry
White matter network
Brain plasticity
Congenital blindness
Corpus callosum

ABSTRACT

Congenital blindness offers a unique opportunity to investigate human brain plasticity. The influence of congenital visual loss on the asymmetry of the structural network remains poorly understood. To address this question, we recruited 21 participants with congenital blindness (CB) and 21 age-matched sighted controls (SCs). Employing diffusion and structural magnetic resonance imaging, we constructed hemispheric white matter (WM) networks using deterministic fiber tractography and applied graph theory methodologies to assess topological efficiency (i.e., network global efficiency, network local efficiency, and nodal local efficiency) within these networks. Statistical analyses revealed a consistent leftward asymmetry in global efficiency across both groups. However, a different pattern emerged in network local efficiency, with the CB group exhibiting a symmetric state, while the SC group showed a leftward asymmetry. Specifically, compared to the SC group, the CB group exhibited a decrease in local efficiency in the left hemisphere, which was caused by a reduction in the nodal properties of some key regions mainly distributed in the left occipital lobe. Furthermore, interhemispheric tracts connecting these key regions exhibited significant structural changes primarily in the splenium of the corpus callosum. This result confirms the initial observation that the reorganization in asymmetry of the WM network following congenital visual loss is associated with structural changes in the corpus callosum. These findings provide novel insights into the neuroplasticity and adaptability of the brain, particularly at the network level.

1. Introduction

Visual experience plays a crucial role in the development of the human brain (Greenough et al., 1987; Kolb, 1998; Li et al., 2022). Brain asymmetry, characterized by discernible disparities in structure and function between the two hemispheres at the local and network levels (Duboc et al., 2015; Rentería, 2012; Toga and Thompson, 2003; Witelson, 1992, 1988), occurs concurrently with the plastic development of the brain (Esteves et al., 2020). Asymmetry is believed to be associated with the specialization of cognitive functions (Toga and Thompson, 2003) within an evolutionary continuum (Fitch and Braccini, 2013). However, our understanding of how visual experience deprivation influences the plastic reorganization of brain asymmetry remains limited. A comprehensive investigation of this issue is crucial for elucidating the plasticity of the human brain and its adaptive developmental processes.

Blindness offers a valuable avenue for investigating the effects of visual loss on brain asymmetry. Visual loss triggers plastic structural and functional reorganization of the brain (Bedny, 2017; López-Bendito et al., 2022), extending to asymmetric structures. Compared with controls with normal sight, early-blind individuals exhibit increased leftward asymmetry in the gray matter structure of the frontal lobe, somatosensory motor areas, and temporal pole. Conversely, increased rightward asymmetry is observed in the visual association cortex (Pan et al., 2008). Early-blind musicians do not exhibit the leftward asymmetry in surface areas of the planum temporale observed in normally sighted musicians (Hamilton et al., 2004). Furthermore, regarding the plastic reorganization of functional asymmetry, existing studies have documented a decreased leftward asymmetry of language processing in individuals with congenital blindness (Lane et al., 2017). An increased rightward asymmetry of spatial processing was observed in various blind cohorts (Cattaneoet al., 2008; Rinaldi et al., 2020), which may be related to the involvement of the right parietal and occipital cortices in spatial tasks (Collignon et al., 2009; Zatorre et al., 2002).

The brain is widely acknowledged as a complex network adhering to

* Corresponding author.
E-mail address: zzhhan@bnu.edu.cn (Z. Han).

https://doi.org/10.1016/j.neuroimage.2024.120844
Received 6 March 2024; Received in revised form 1 September 2024; Accepted 8 September 2024
Available online 10 September 2024

the small-world property and characterized by highly connected hubs and modules (Bullmore and Sporns, 2009). This configuration enables efficient information transmission between neurons while maintaining a high degree of local connectivity, which is crucial for supporting intricate cognitive functions (Park and Friston, 2013). In the white matter (WM) structural network, gray matter regions serve as nodes, and WM connections between brain regions act as edges (Gong et al., 2009a, 2009b). Investigating the patterns of the white matter network provides crucial evidence for understanding the structure and function of the human brain (Sporns, 2013). Previous studies on WM network in blind individuals have revealed reorganization of topological properties (Li et al., 2013; Shu et al., 2009b; Zhou et al., 2022) and cross-modal cognitive functions. Specifically, decrease in network efficiencies (Li et al., 2013; Shu et al., 2009b; Zhou et al., 2022), fiber numbers (FNs; Bauer et al., 2017), and increase in characteristic path length (Shu et al., 2009b; Zhou et al., 2022) were observed in blind individuals. And the structural networks of blinds involved in the processing of motor, somatosensory, tactile information, and braille reading (Jiao et al., 2023; Shu et al., 2009b). Moreover, the increased network efficiencies in glaucoma indicated that the degree and onset of visual impairment influenced topological properties of WM network (Di Ciò et al., 2020).

In recent years, advancements in diffusion tensor imaging technology and graph theory analysis methods (Sporns, 2018) have facilitated the examination of hemispheric brain WM network models to depict brain asymmetry at the network level (Wei et al., 2018; Zhao et al., 2019; Zhong et al., 2021, 2016). These models involve calculating and comparing differences in topological metrics between hemispheric WM networks. Normal individuals showed significant leftward asymmetry in network efficiencies of both binary (Caeyenberghs and Leemans, 2014) and streamline density weighted (Sun et al., 2017) WM networks. Conversely, a developmental study indicated rightward asymmetry in network efficiency of connectivity probability weighted WM network in adolescents and young adults (Zhong et al., 2016). The inconsistent findings might be due to variations in network construction methods (Bassett et al., 2011; Yang et al., 2017; Zalesky et al., 2010; Zhong et al., 2016, 2015). Finally, this research methodology has been used to investigate brain asymmetry of network efficiencies in patients. Individuals with autism spectrum disorder exhibited a rightward asymmetry in network local efficiency, while network global efficiency remained symmetrical (Wei et al., 2018). And asymmetry in network efficiencies increased in patients with schizophrenia (Zhu et al., 2021). However, the asymmetry of WM networks in blind individuals remains unclear. Discussing this issue will enhance our understanding of how visual experience shapes brain plasticity.

The structure of interhemispheric WM connections reflects, drives, and maintains structural and functional brain asymmetries (Voineskos et al., 2010). The corpus callosum (CC), the critical bundle of the WM pathway for interhemispheric brain communication (Bloom and Hynd, 2005; Spillane, 1960), directly influences cortical connection establishment and brain neurodevelopment (Aboitiz et al., 1992; Alberto Marzi, 2010; Szczupak et al., 2023; Theofanopoulou, 2015), playing a pivotal role in brain asymmetry. A previous developmental study on prenatal human brains with agenesis of the CC revealed a more symmetric configuration in the temporal lobe and an increased frequency of abnormal asymmetric patterns (Schwartz et al., 2021). Disrupted asymmetry in the prefrontal cortex of children with attention-deficit/hyperactivity disorder was associated with anomalous growth in the anterior CC (Gilliam et al., 2011). Similar findings were observed in patients with dyslexia, in which asymmetry of the temporal plane and morphology of the CC were implicated (Beaton, 1997). Additionally, regarding functional hemispheric asymmetry, the leftward frontal cortical asymmetry of anger and aggression in the prefrontal lobe (Schutter and Harmon-Jones, 2013) and the leftward asymmetry of auditory perception involved in dichotic listening studies (Westerhausen and Hugdahl, 2008) were related to the CC. Importantly, significant structural and functional reorganization in the CC has been observed in individuals with visual loss or damage (Aguirre et al., 2016; Cavaliere et al., 2020; Celeghin et al., 2017; Jiao et al., 2023; Shi et al., 2015; Tomaiuolo et al., 2014). The structural alterations in blind individuals mainly occurred in the splenium part of CC, which reduced in various structural measures, including WM volume (WMV; Cavaliere et al., 2020; Ptito et al., 2008), cortical thickness (Leporé et al., 2010; Shi et al., 2015), surface area (Cavaliere et al., 2020; Tomaiuolo et al., 2014), FNs (Cavaliere et al., 2020), and diffusion measures (Aguirre et al., 2016; Jiao et al., 2023). And the curvature of CC was showed a decrease in blindness (Tomaiuolo et al., 2014). Moreover, The CC was involved in the braille reading induced by congenital visual loss (Jiao et al., 2023).

However, the previous studies in blindness primarily focused on plasticity changes in asymmetry of local structures with limited exploration at the network level, particularly the WM structural network. Additionally, investigations into structural asymmetry predominantly concentrated on early-blind populations, challenging the elimination of the impact of visual experience and compromising the study's purity. Moreover, there is a lack of understanding regarding the physiological mechanisms underlying brain network asymmetry, such as its association with the structural reorganization of interhemispheric WM connections (i.e., the CC). To address these issues, our study recruited congenitally blind participants who lost their vision from birth and did not have any visual experiences during brain cortical development. We focused on the WM structural network of the brain hemispheres utilizing diffusion tensor imaging technology and graph theory analysis methods to investigate changes in the topological properties of the WM network in the hemispheres. Simultaneously, we employed a WM atlas with detailed segmentation of the CC for voxelwise analysis. This analysis aimed to explore whether the reorganization of hemispheric asymmetry is accompanied by structural reorganization of interhemispheric WM tracts, providing a physiological mechanism-based explanation for asymmetry reorganization (Fig. 1).

2. Materials and methods

2.1. Participants

Our study recruited 21 participants with congenital blindness (CB, age 24.38 ± 5.32 years old, 7 female) and 21 normally sighted controls (SCs, age 22.81 ± 2.58 years old, 11 female). The two groups were well matched for age [two-tailed two-sample *t*-test: $t_{(40)} = 1.22$, $P = 0.23$] and sex [two-tailed Pearson *chi-square* test: $\chi^2_{(1)} = 0.89$, $P = 0.35$].

The CB participants had blindness of peripheral origin from birth, with the etiology attributed to factors such as eyeball dysplasia, fundus dysplasia, macular dysplasia, optic nerve atrophy, retinopathy of prematurity, and retinitis pigmentosa. The participants self-reported that they had never been able to distinguish colors, shapes, or motion, while 13 of them self-reported that they had minimal light perception. The sighted participants had normal or corrected-to-normal vision.

All participants were right-handed (Oldfield, 1971), were native Chinese speakers, and reported no known neurological or psychiatric problems. They received compensation for their participation and provided informed written consent. This study received full ethical approval from the Institutional Review Board of the National Key Laboratory of Cognitive Neuroscience and Learning, Beijing Normal University.

2.2. MRI data acquisition

MRI scans were acquired on a 3T Siemens Prisma scanner at the Imaging Center for Brain Research, Peking University. T1-weighted images and diffusion-weighted images (DWIs) were collected. For high-resolution T1-weighted images, 192 slices per slab were obtained through sagittal acquisition utilizing a magnetization-prepared rapid gradient-echo (MP-RAGE) sequence with the following imaging parameters: echo time (TE) = 2.98 ms; repetition time (TR) = 2530 ms;

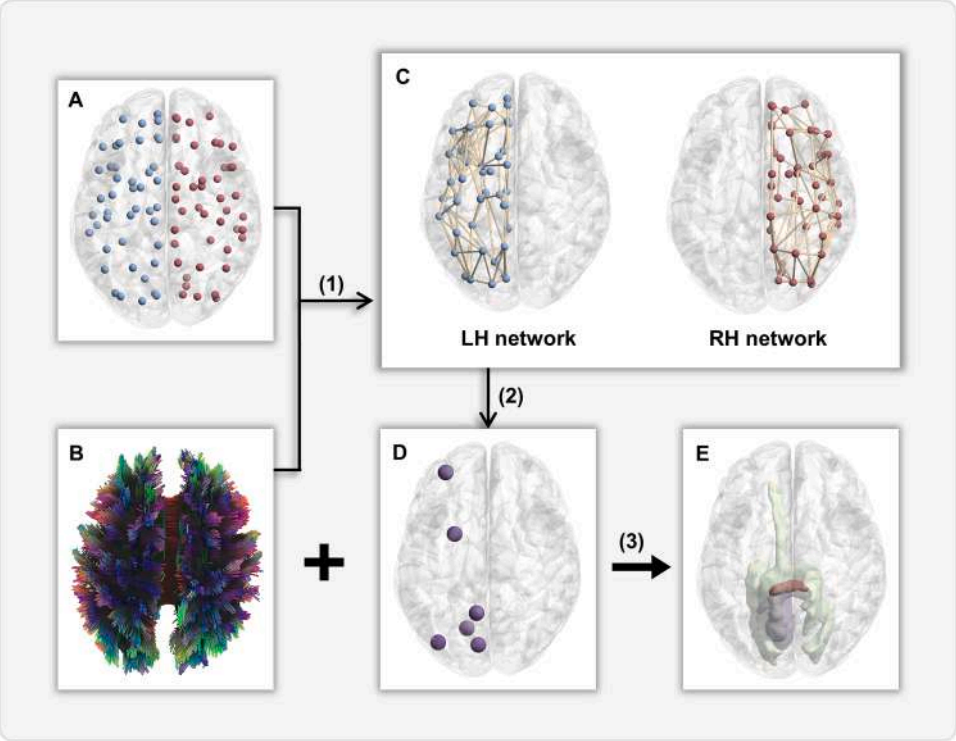

Fig. 1. Schematic flowchart for the data analysis. (1) The automated anatomical labeling (AAL) template (A) was utilized to construct hemispheric white matter networks (C), initially by reconstructing the entire brain's white matter fibers (B) through deterministic fiber tractography. (2) Identification of key brain nodes exhibited significant group differences in nodal efficiency (D) which were associated with topological asymmetry in hemispheric white matter networks. (3) Analysis of the interhemispheric tracts (E) connecting the key nodes. LH, left hemisphere; RH, right hemisphere.

inversion time (TI) = 1100 ms; slice thickness = 1 mm; voxel size = 0.5 × 0.5 × 1.0 mm^3; flip angle = 7°; and field of view (FOV) = 256 × 256 mm^3. For the DWIs, axial acquisition was conducted using a single-shot echo-planar imaging (EPI) sequence. The integral parallel acquisition technique (iPAT) was employed with an acceleration factor of 2 to reduce the acquisition time. The detailed parameters were as follows: 70 axial slices covering the whole brain; TE = 73 ms; TR = 5100 ms; diffusion directions = 30; b-value 1 = 0 s/mm^2; b-value 2 = 1000s/mm^2; b-value 3 = 2000s/mm^2; slice thickness = 2 mm; voxel size = 2.0 × 2.0 × 2.0 mm^3; flip angle = 60°; and FOV = 224 × 224 mm^2.

2.3. MRI data preprocessing

The T1-weighted images were preprocessed utilizing Statistical Parametric Mapping version 12 (http://www.fil.ion.ucl.ac.uk/spm/software/spm12/) with default parameters incorporating the Diffeomorphic Anatomical Registration Through Exponentiated Lie Algebra (DARTEL) algorithm (Ashburner, 2007). First, the T1-weighted images were segmented into three parts [i.e., gray matter (GM), WM, and cerebrospinal fluid]. Second, the segmented WM images were resampled to 1.5 × 1.5 × 1.5 mm^3 and spatially normalized to Montreal Neurological Institute (MNI) standard space. Third, the normalized WM images were modulated by the Jacobian determinants generated during spatial normalization to obtain volume measurements (Ashburner and Friston, 2000; Goldszal et al., 1998). Finally, the modulated, normalized WMV images were smoothed with a Gaussian kernel of 4 mm full width at half maximum, and the resulting WMV images were used in the following analysis.

The DWIs were preprocessed using PANDA, a pipeline tool for analyzing brain diffusion images (Cui et al., 2013) (http://www.nitrc.org/projects/panda/). The image processing procedure comprised (i) brain extraction with skull removal and cropping gap; (ii) correction for simple head motion, eddy current distortions, and b-matrix (Leemans and Jones, 2009); (iii) voxelwise computations for tensor matrix and diffusion tensor metrics [i.e., fractional anisotropy (FA), axial diffusivity (AD), mean diffusivity (MD) and radial diffusivity (RD)]; and (iv) image normalization to MNI standard space and smoothing with a 6 mm Gaussian kernel.

2.4. Hemispheric WM network construction

To investigate the impact of blindness on brain network asymmetry, two hemispheric WM networks were constructed for each subject. The schematic flowchart for network construction is shown in Fig. 1. Like other complex networks, the brain network is composed of two basic elements: nodes and edges. Based on the previous studies on the WM network in blindness (Jiao et al., 2023; Li et al., 2013; Shu et al., 2009b, 2009a; Wang et al., 2017; Zhou et al., 2022), We determined the current method of constructing hemispheric WM network, and described the detailed procedures below.

2.4.1. Definition of nodes in hemispheric WM networks

We defined the nodes of the brain network utilizing the automated anatomical labeling (AAL) template (Tzourio-Mazoyer et al., 2002) without the cerebellum. This atlas comprises a total of 90 brain regions that are evenly distributed across both hemispheres. Consequently, each hemisphere was parcellated into 45 regions, and each region served as a node of the hemispheric WM network. For each subject, the original AAL in MNI standard space was first transformed into the individual's native diffusion space using FSL (http://www.fmrib.ox.ac.uk/fsl). Briefly, a linear transformation was performed between the individual T1-weighted image and the individual FA image in the native diffusion space. Then, the native T1-weighted image was nonlinearly registered to the T1 template of ICBM152 in the MNI standard space. Finally, the two resulting inverse transformations were applied to the AAL in MNI space, resulting in a subject-specific gray matter parcellation with 90 regions in

the native diffusion space for subsequent fiber tracking (i.e., 45 regions for each hemisphere).

2.4.2. WM tractography for hemispheric WM networks

Deterministic fiber tractography, which is a commonly utilized methodology for inferring connections between nodes, was used to determine whether two GM nodes were anatomically connected (Van Den Heuvel and Sporns, 2011; Wang et al., 2018; Zhong et al., 2015). The fiber assignment by continuous tracking (FACT) algorithm (Mori et al., 1999; Mori and van Zijl, 2002) was utilized to reconstruct all the WM fibers in the whole brain. Fiber tractography was terminated if/when the crossing angle of two consecutive orientations was greater than 45° or the FA value was less than 0.2.

2.4.3. Edge definition for hemispheric WM networks

The weighted edge linking each pair of GM nodes was calculated as the total FN connecting two GM nodes, which was computed by aggregating the existing streamlines connecting the two regions. The FN offers insights into the quantity of WM connectivity between two GM regions. The seed and target regions in the hemispheric network were restricted within the same hemisphere. By employing this approach, two separate 45×45 symmetric weighted matrices were obtained for each subject, with each network representing a hemispheric network within the human brain. To remove spurious connections due to imaging noise, head motion, or cumulative tractography errors, we excluded edges that existed in less than 80% of the subjects and for which the FN was less than 3 (Li et al., 2009; Shu et al., 2011; Xu et al., 2021; Zhang et al., 2023), especially in researches recruited the blind participants (Li et al., 2013; Shu et al., 2009b; Zhou et al., 2022). We test the effects of different threshold values from 1 to 5 on network properties, and finally determined the most appropriate FN threshold value of 3 (Li et al., 2013, 2009; Shu et al., 2011; see Supplementary Analysis 1 for further details).

2.5. Topological metrics of hemispheric networks

Graph theory analysis provides a valuable opportunity to investigate the topological properties of WM structural networks (Bullmore and Sporns, 2009). To understand the overall structure of the whole network as well as the information transfer properties between nodes, network global efficiency (E_g) and network local efficiency (E_{loc}), which are two widely used metrics to characterize network-level efficiency (M. Li et al., 2021; Wei et al., 2018; Zhao et al., 2019; Zhong et al., 2016, 2021) that also involve the efficiency of information transmission between nodes in the network (Duda et al., 2014; Latora and Marchiori, 2001; Van Mieghem, 2023; Zhou and Wang, 2018), were calculated. At the nodal level, the corresponding metric was nodal local efficiency ($E_{loc\text{-}nodal}$). These nodal metrics can be used to understand the centrality of nodes and the information transmission characteristics within complex network structures. All three metrics mentioned above were the main focus of this study and were calculated within the same hemisphere by using the Gretna package (Wang et al., 2015).

2.5.1. E_g

E_g is a global metric used to measure the overall communication efficiency of parallel information transfer in a network, and a higher value means that it is easier and faster to transfer information between the nodes in the network. E_g is calculated as the mean of the reciprocal of the shortest path between all pairs of nodes in the network (Latora and Marchiori, 2001):

$$E_g^G = \frac{1}{N(N-1)} \sum_{i \in G} \sum_{j \neq i \in G} \frac{1}{L_{ij}}$$

where L_{ij} is the shortest path length between nodes i and j, and N is the number of nodes in graph G.

2.5.2. E_{loc}

E_{loc} represents the communication efficiency of information transfer within the local environment, which reflects the average ability of a network to tolerate faults by measuring the communication efficiency among the nearest neighbors of the node when it is removed. This metric is defined as follows (Latora and Marchiori, 2001):

$$E_{loc}^G = \frac{1}{N} \sum_{i \in G} E_g^{G_i}$$

where G_i is the neighborhood subnetwork of node i composed of the nearest neighbors and their connections, and N is the number of nodes in graph G_i.

2.5.3. $E_{loc\text{-}nodal}$

$E_{loc\text{-}nodal}$ represents the information communication capacity of a particular node within the subnetwork composed of its nearest neighbors and their connections. For a particular node i, the computational formula is as follows:

$$E_{loc-nodal}^G(i) = E_g^{G_i}$$

where G_i denotes the neighborhood subnetwork of node i.

2.6. Asymmetry index (AI)

The AIs of network-level efficiency metrics (i.e., E_g and E_{loc}) were calculated to measure the differences in information transfer efficiency between the two hemispheres. To characterize the degree of asymmetry, we computed the AIs of the E_g and E_{loc} metrics for each subject using the following formula:

$$AI = \frac{E(L) - E(R)}{E(L) + E(R)}$$

where $E(L)$ and $E(R)$ represent the E_g or E_{loc} of the whole left and right hemispheric networks, respectively. A positive AI indicates leftward asymmetry of the brain, while a negative AI indicates rightward asymmetry.

2.7. Interhemispheric connections related to the plastic reorganization of hemispheric asymmetry

In the above analysis, we found that the reorganization of hemispheric asymmetries in blind individuals was related to the "damage" of some key nodes in the left hemisphere, as demonstrated by the decreased transfer efficiency of the intrahemispheric connections of these key nodes. To further explore whether changes in asymmetry are accompanied by structural alterations in interhemispheric WM connections, we employed the deterministic fiber tractography method, which is the same as that used in network construction, to determine the interhemispheric connections passing through each identified key node. The CC is the main fibrous bundle responsible for interhemispheric information transfer; hence, the interhemispheric connections passing through each key node were determined by all the fibers passing through or terminating in both the key node and the CC. We merged all five CC subdivisions in the International Consortium of Brain Mapping DTI-based atlas obtained from 81 normal subjects (ICBM-DTI-81) (Mori et al., 2008) to define the CC region. The ICBM-DTI-81 atlas is composed of 50 subdivisions, including five segments of the CC: the genu (GCC), the body (BCC), the splenium (SCC), the left tapetum, and the right tapetum. The WMV values of the interhemispheric connections were compared between groups to investigate the structural changes.

2.8. Statistical analysis

2.8.1. Blindness-relevant changes in asymmetry of network-level efficiencies

To identify the network-level efficiencies (E_g and E_{loc}) of hemispheric networks that were influenced by blindness, a two-way mixed-design analysis of covariance (ANCOVA) was conducted. This analysis involved two levels for vision (blind vs. sighted) * two levels for the hemispheric network used as the repeated variable (left hemisphere vs. right hemisphere), with sex and hemispheric intracranial volume (IV) considered additional covariates for each network-level efficiency (Barnes et al., 2010; Yan et al., 2011). The IV was calculated as the sum of the normalized, modulated, smoothed tissue segments (GM + WM + cerebrospinal fluid). To further reveal the pattern of the alterations in each metric, post hoc two-tailed two-sample *t* tests were performed. The false discovery rate (*FDR)* correction ($P < 0.05$) was employed in both the ANCOVA and post hoc tests to correct for multiple comparisons (Genovese et al., 2002).

2.8.2. Blindness-relevant changes in the AI of network-level efficiencies

To evaluate whether and how visual loss influences the asymmetries of WM networks, permutation correction was applied to evaluate the significant differences in the residual AI values of E_g and E_{loc} between the two groups. Specifically, we conducted a permutation test to compare the mean difference of the residual AI values against a null distribution generated with a decoding procedure repeated 1000 times, controlling for the influences of sex and total IV, and with the differences in hemispheric IV (calculated as left–right) serving as covariates. Then, the distribution was fitted with a generalized Pareto distribution by the MATLAB package EPEPT (Knijnenburg et al., 2009). Finally, the difference was considered statistically significant if $P < 0.05$.

2.8.3. Blindness-relevant changes in nodal-level properties of the left hemisphere

Based on the results of the above analysis, we found that congenital blindness significantly altered the AI of the E_{loc}, which was related to the reduction in the residual E_{loc} in the left hemisphere. To further explore the "damage" of the key nodes leading to the reduction in the residual E_{loc} of the left hemisphere in blind individuals, in the nodal-level analysis, we focused on the nodes with significant group differences in nodal-level topological metrics in the CB group restricted to the left hemisphere. For $E_{loc\text{-}nodal}$, after controlling for the influence of sex and left hemispheric IV, we statistically compared the residual values between the CB and SC groups using permutation tests to evaluate the group differences (1000 times, $P < 0.05$). The nodes exhibited significant group differences in left hemisphere were defined as the key nodes.

Moreover, in order to reveal the blindness-relevant changes in intrahemispheric WM connections of key nodes, we evaluated the group differences in WM connectivity strength. Specifically, for each existing intrahemispheric connection of each key node, we extracted the residual FN (after regressing out sex and left hemispheric IV), and performed permutation test (1000 times, $P < 0.05$) in residual FN between two groups.

2.8.4. Blindness-relevant structural changes in interhemispheric connections related to the plastic reorganization of hemispheric asymmetry

To identify the interhemispheric WM tracts that were connected to the aforementioned "damaged" key nodes and influenced by blindness, we conducted a voxelwise two-sample *t*-test for the residual WMVs after controlling for sex and total IV for each node. *FDR* correction ($P < 0.001$, cluster size > 50 voxels) was utilized within a WM mask for the WM tract connecting each node. The mask was generated by summing the voxels (in which no less than 20% of subjects had fibers) containing WM fibers across each group. Post hoc two-tailed two-sample *t* tests were performed to clarify the pattern of the structural changes in the mean residual WMV of each significant tract (*FDR* corrected, $P < 0.001$).

Then, we used ICBM-DTI-81 (Mori et al., 2008) to define WM tracts with significant group differences. We defined each significant tract by calculating the overlap between the tract and each subdivision in the ICBM-DTI-81 atlas. The overlap index (OI) was computed as the ratio of the number of overlapping voxels to the number of voxels in the significant WM cluster. The WM cluster was labeled according to the subdivision with the highest OI in the atlas.

3. Results

3.1. Blindness-relevant changes in asymmetry of network-level efficiencies

Two-way ANCOVA (covarying for sex and hemispheric IV) used to analyze the network-level efficiencies, and the asymmetries in residual E_g and residual E_{loc} for both groups are illustrated in Fig. 2.

For the residual E_g metric (Fig. 2A), there was only a significant main effect of hemisphere [$F_{(1,40)} = 68.37$, *FDR* corrected $P < 0.001$] but no interaction effect [$F_{(1,40)} = 0.07$, *FDR* corrected $P = 0.79$] or main effect of vision [$F_{(1,40)} = 1.32$, *FDR* corrected $P = 0.26$]. Specifically, we obtained a detailed description of the changing patterns for the residual E_g in the hemispheric networks of the two groups via post hoc analysis. Regarding within-group asymmetry, significant leftward (i.e., left > right) hemispheric asymmetry in residual E_g was observed both in the CB [$t_{(20)} = 6.12$, *FDR* corrected $P < 0.001$] and in SC [$t_{(20)} = 5.64$, *FDR* corrected $P < 0.001$] groups. There were no significant differences in asymmetry of the two hemispheres between groups [left hemisphere: $t_{(40)} = 1.13$, *FDR* corrected $P = 0.32$; right hemisphere: $t_{(40)} = 1.00$, *FDR* corrected $P = 0.32$].

For the residual E_{loc} metric (Fig. 2B), a significant interaction effect [$F_{(1,40)} = 6.05$, *FDR* corrected $P = 0.03$] and main effect of hemisphere [$F_{(1,40)} = 16.43$, *FDR* corrected $P < 0.001$] were observed, but the main effect of vision did not reach significance [$F_{(1,40)} = 2.25$, *FDR* corrected $P = 0.14$]. Regarding within-group asymmetry, there was significant leftward (i.e., left > right) hemispheric asymmetry in the SC group [$t_{(20)} = 4.09$, *FDR* corrected $P < 0.001$] but no asymmetry in the CB group [$t_{(20)} = 1.32$, *FDR* corrected $P = 0.27$]. Regarding the between-group differences in asymmetry, the residual E_{loc} of the left hemispheric network in the CB group was significantly lower than that in the SC group [$t_{(40)} = 2.62$, *FDR* corrected $P = 0.02$], while the difference in the right hemispheric network between the two groups was not significant [$t_{(40)} = 0.38$, *FDR* corrected $P = 0.71$].

The results revealed a significant leftward asymmetry in the residual E_g of hemispheric networks for both groups. However, there were no significant group differences, indicating that the E_g metric is not highly sensitive to visual factors and that the asymmetry in E_g remained unaffected by visual deprivation in congenital blindness patients. In contrast, we observed a significant leftward asymmetry in E_{loc} in the SC group, while the asymmetry in the congenitally blind group showed significant rightward movement, reaching symmetry. Compared with that in the SC group, the observed change in the asymmetry of E_{loc} was attributed to the reduction in E_{loc} of the left hemispheric network in the CB group. E_{loc} is a network efficiency metric calculated based on the local network of nodes, and we hypothesize that this outcome may suggest alterations in some critical nodes of the left hemisphere network in the congenitally blind group, leading to these changes.

3.2. Blindness-relevant changes in AI of network-level efficiencies

The group difference in the residual AI of E_g did not reach significance (permutation test, $P = 0.42$), while a significant group difference was observed for the residual AI of E_{loc} (permutation test, $P = 0.03$) between the CB and SC groups, as shown in Fig. 3. Specifically, for E_{loc}, compared with the SC group, the CB group exhibited a decrease in the residual AI. According to the above post hoc test of the ANCOVA of the residual E_{loc} (Fig. 2B), the residual E_{loc} of the left hemispheric network in the CB group decreased significantly compared with that in the SC

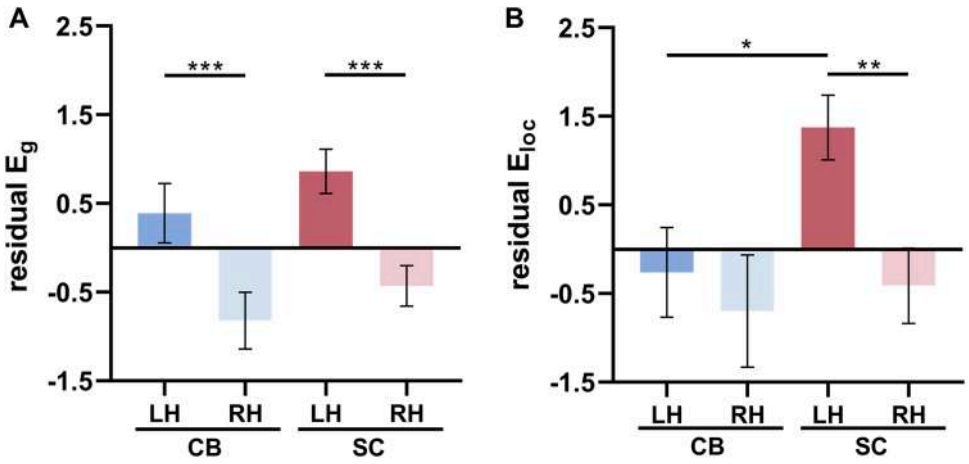

Fig. 2. Asymmetry in the residual network local efficiency (A: E_{loc}) and global efficiency (B: E_g) of the hemispheric networks for each group after controlling for sex and hemispheric intracranial volume. Error bars indicate the standard error of the mean. *FDR* corrected ($q < 0.05$): $^*P < 0.05$; $^{**}P < 0.01$; $^{***}P < 0.001$. CB, congenital blindness; LH, left hemisphere; RH, right hemisphere; SC, sighted control.

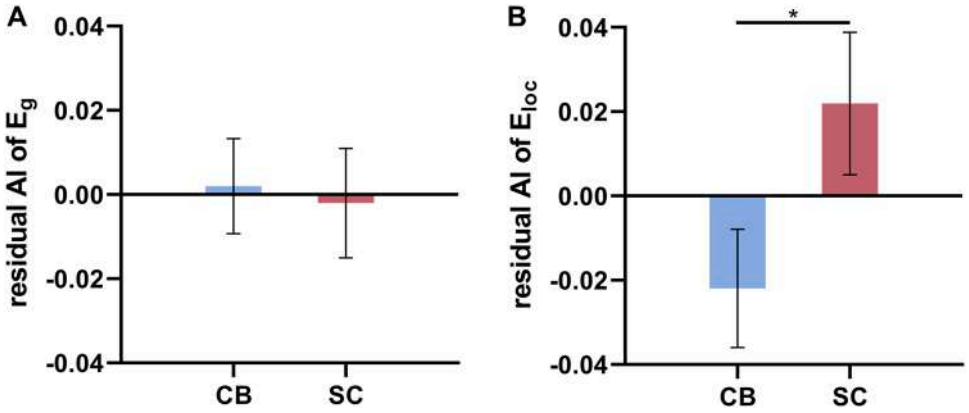

Fig. 3. Group comparisons of the residual asymmetry index (AI) in terms of network local efficiency (A: E_{loc}) and global efficiency (B: E_g) for the hemispheric networks after controlling for sex, total intracranial volume, and differences in hemispheric intracranial volume. Error bars indicate the standard error of the mean. Corrected for permutation test: $^*P < 0.05$. CB, congenital blindness; SC, sighted control.

group, but there were no differences in the residual E_{loc} of the right hemispheric network.

The analyses of residual AI values were consistent with the results of the ANCOVA. Particularly in terms of E_{loc}, the SC group exhibited a leftward asymmetry of the WM network; however, the asymmetry in the CB group moved significantly rightward to achieve a symmetric state.

3.3. Blindness-relevant changes in nodal-level properties of left hemisphere

According to the above asymmetry analysis, we found that a reduction in E_{loc} in the left hemisphere led to a change in the asymmetry of the WM network in the CB group. Therefore, we conducted an in-

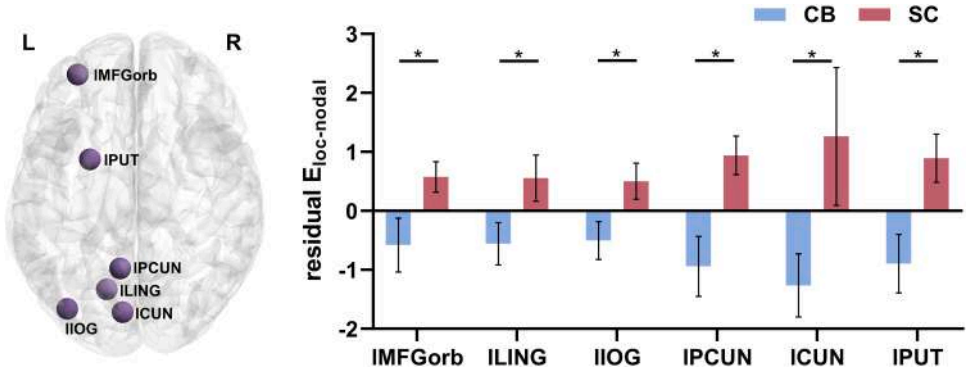

Fig. 4. Key brain nodes with significant group differences in the residual nodal local efficiency ($E_{loc\text{-}nodal}$) for the left hemispheric network after controlling for sex and left hemispheric intracranial volume. Error bars indicate the standard error of the mean. Corrected for permutation test: $^*P < 0.05$. CB, congenital blindness; CUN, cuneus; IOG, inferior occipital gyrus; l/L, left hemisphere; LING, lingual gyrus; MFGorb, orbital part of middle frontal gyrus; PCUN, precuneus; PUT, putamen; R, right hemisphere; SC, sighted control.

depth analysis to investigate whether these alterations were induced by "damage" to some key nodes in the left hemisphere. There were six regions in the left hemisphere that exhibited significant group differences. Specifically, compared to the SC groups, all these six nodes showed notable reduction in residual $E_{loc\text{-}nodal}$ values in the CB group (Fig. 4): the left orbital part of the middle frontal gyrus (lMFGorb; permutation test, $P = 0.04$), the left lingual gyrus (lLING; permutation test, $P = 0.04$), the left inferior occipital gyrus (lIOG; permutation test, $P = 0.05$), the left precuneus (lPCUN; permutation test, $P = 0.02$), the left cuneus (lCUN; permutation test, $P = 0.02$), and the left putamen (lPUT; permutation test, $P = 0.02$).

Moreover, the following intrahemispheric connections of key nodes showed significant blindness-relevant changes (Fig. 5): lLING-lPCUN connection (permutation test, $P = 0.003$), lLING-left calcarine fissure connection (lLING-lCAL connection; permutation test, $P = 0.01$), lPCUN-lCAL connection (permutation test, $P = 0.002$), lPCUN-lPHG connection (permutation test, $P = 0.03$), lCUN-lCAL connection (permutation test, $P = 0.006$), lPUT-left dorsolateral part of superior frontal gyrus connection (lPUT-lSFGdor connection; permutation test, $P = 0.02$). Compared with the SC group, the connectivity strength of lPUT-lSFGdor connection increased in CB group, while all other connections decreased.

For various nodal properties in left hemisphere, the nodes that exhibited significantly decreased values in the CB group were concentrated in specific brain regions, such as the occipital regions, a few frontal regions, and the subcortical putamen. Notably, most key nodes and their intrahemispheric connections with significant differences were in the occipital lobe, where visual information is processed in sighted individuals.

3.4. Blindness-relevant structural changes in the interhemispheric connections related to the plastic reorganization of hemispheric asymmetry

For each key node defined in the above analysis, we performed a voxelwise two-sample *t*-test (*FDR* corrected, $q < 0.001$; cluster size > 50 voxels) for the residual WMV of the interhemispheric tract connecting the key node between the two groups. The residual WMVs of the interhemispheric tracts connecting the lLING and lPCUN showed significant group differences (Table 1, Fig. 6). The tracts passing through the lLING and lPCUN had the only and largest OI with the SCC (Fig. 6A) in the ICBM-DTI-81 atlas. Specifically, in the post hoc two-sample *t*-test analysis, the mean residual WMVs for both tracts in the CB group were significantly lower than those in the SC group [lLING-SCC: $t_{(40)} = 5.99$, lPCUN-SCC: $t_{(40)} = 6.01$; *FDR* corrected $Ps < 0.001$] (Fig. 6B, 6C). The results demonstrated that reorganization of brain asymmetry in blind individuals was accompanied by changes in the structure of interhemispheric WM connections.

4. Discussion

Through the analysis of individuals with congenital blindness, our study revealed the influence of congenital visual experience deprivation on the plasticity of the topological asymmetry of the hemispheric WM network. Additionally, we concurrently observed the relationship between the plastic reorganization of topological asymmetry and structural changes in the interhemispheric WM connections. Specifically, we first observed a symmetrical state for the network local efficiency (E_{loc}) in individuals with congenital blindness compared to the significant leftward asymmetry in sighted individuals. Second, the plastic change in asymmetry in individuals with congenital blindness was due to the "damage" of key nodes and their intrahemispheric connections within the left hemisphere, with these nodes distributed across multiple areas in the occipital lobe, parts of the frontal lobe and subcortical cortex. Finally, the interhemispheric WM tracts connecting these key nodes underwent structural reorganization in the SCC. Overall, the "damage" to key nodes in the left hemisphere of individuals with congenital blindness triggered a plastic reorganization of brain asymmetry, and the physiological mechanism of this reorganization of asymmetry might involve changes in the structure of the CC.

4.1. Plastic reorganization of topological asymmetry in the hemispheric WM network

In the analysis of complex networks using graph theory, E_{loc} and E_g play a vital role in characterizing the properties related to information transmission and overall connectivity of networks (Duda et al., 2014; Latora and Marchiori, 2001; M. Li et al., 2021; Van Mieghem, 2023; Zhou and Wang, 2018). In this study, the observed significant leftward asymmetries in the network efficiencies of hemispheric WM networks for sighted individuals were consistent with those of previous studies (Caeyenberghs and Leemans, 2014; Cai et al., 2019; Dennis et al., 2013; Nucifora et al., 2005; Ratnarajah et al., 2013; Sun et al., 2017), indicating enhanced integration within the left hemisphere as opposed to the right hemisphere. The pronounced leftward asymmetries in sighted individuals may be related to the lateralization of cognitive functions (e.g., visual word recognition, reading, and sentence processing) to the left hemisphere (Binder et al., 1997; Caeyenberghs and Leemans, 2014; Chiarello et al., 2013; Labache et al., 2020; Qiu et al., 2011). However, for individuals with congenital blindness, the topological metric of E_{loc} reorganized to a symmetrical state, while the leftward asymmetry of E_g remained. These findings highlight the neural plasticity of the brain in response to long-term visual deprivation, providing substantial evidence for understanding how the brain reorganizes to adapt to changes in sensory input at the network level.

Compared to sighted individuals, E_{loc} of congenitally blind patients shifted from significant leftward asymmetry to a symmetrical state. Post hoc comparisons revealed that this was due to the reduction in E_{loc} in the left hemisphere of blind individuals. This was consistent with previous studies on gray matter structural asymmetry, blind individuals exhibited a reduction on the left visual association cortex (Pan et al., 2008) and left planum temporale (Hamilton et al., 2004). E_{loc} measures the tightness of connections between nodes in a network (Barmpoutis and Murray, 2011), which signifies the efficiency of information transmission between neurons in a specific subnetwork (Barmpoutis and Murray, 2011; Caccetta, 1979; Latora and Marchiori, 2001). A high local efficiency may indicate faster and more effective information transmission within the local subnetwork (Latora and Marchiori, 2001). Therefore, we speculated that the reduction in E_{loc} in the left hemisphere in individuals with congenital blindness might be related to changes in cognitive functions associated with altered sensory input (Binder et al., 1997; Caeyenberghs and Leemans, 2014; Chiarello et al., 2013; Labache et al., 2020; Qiu et al., 2011). This change reflected a decrease in the efficiency of information transmission for visual perception, motor control, and specific cognitive functions (such as language), which are tightly coupled with visual information (Binder et al., 1997; Chiarello et al., 2013; Labache et al., 2020; Qiu et al., 2011). The leftwards functional lateralization of language was found significantly reduced in blind individuals (Lane et al., 2017). While there were evidences showed that new cognitive functions (e.g. auditory, tactile, syntactic processing) (Jiao et al., 2023; Kim et al., 2017; Lin et al., 2022) were invloved and enhancement of functional connectivity (Abboud and Cohen, 2019; Lin et al., 2022; Tian et al., 2024) in left occipital cortex of blind individuals. However, these "increase" were not sufficient to offset the "decreased" induced by visual loss, which was similar with our findings. The increased connectivity strength of lPUT-lSFGorb connection was not strong enough to save the widely reduction in the occipital connections (Fig. 5).

Notably, E_{loc} in the right hemisphere did not decrease in blind individuals. This was possibly due to their reliance on tactile and auditory information to complete cognitive tasks, which enhanced the spatial perception (Aliotti, 1981; Carota and Bogousslavsky, 2018; Cona and Scarpazza, 2019), musical (Bosnar-Puretic et al., 2009; Koelsch et al., 2005; Vaquero et al., 2018), and artistic (Nikolaenko, 1998) functions

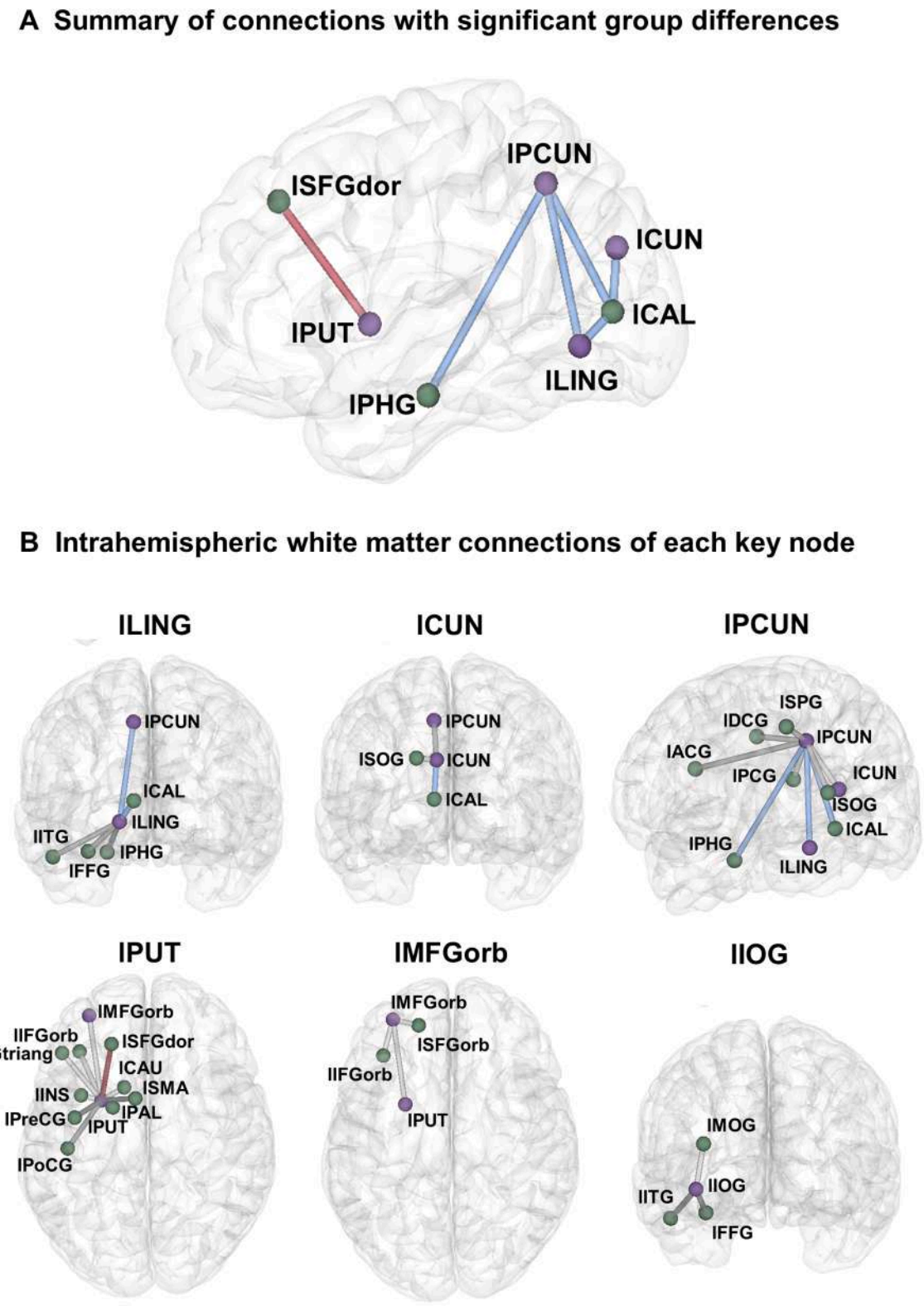

Fig. 5. Group comparisons of the residual fiber number of intrahemispheric connections for key nodes after controlling sex and left hemispheric intracranial volume. The intrahemispheric connections with significant group differences (A) were summarized from the group comparison for each key node (B). The nodes (purple, the key nodes; green, the nodes peripheral to the key nodes) and the intrahemispheric connections (blue, the connections with significant decreased connectivity strength in CB; red, the connections with significant increased connectivity strength in CB; gray, the existing connections without group differences) were shown in different colors. ACG, anterior cingulate and paracingulate gyri; CAL, calcarine fissure; CAU, caudate nucleus; CB, congenital blindness; CUN, cuneus; DCG, median cingulate and paracingulate gyri; FFG, fusiform gyrus; IFGorb, orbital part of inferior frontal gyrus; IOG, inferior occipital gyrus; ITG, inferior temporal gyrus; INS, insula; l, left hemisphere; LING, lingual gyrus; MFGorb, orbital part of middle frontal gyrus; MOG, middle occipital gyrus; PAL, pallidum; PCG, posterior cingulate gyrus; PCUN, precuneus; PHG, parahippocampal gyrus; PoCG, postcentral gyrus; PreCG, precental gyrus; PUT, putamen; SFGdor, dorsolateral part of superior frontal gyrus; SFGorb, orbital part of superior frontal gyrus; SMA, supplementary motor area; SOG, superior occipital gyrus; SPG, superior parietal gyrus.

Table 1
Interhemispheric white matter tracts with significant group differences passing through each seed node according to two-sample t-test analysis of residual white matter volumes.

Seed node	Label of white matter tract	*x*	*y*	*z*	Cluster size	t value
Left lingual gyrus (lLING)	Splenium of the corpus callosum (SCC)	0	−34	6	57	9.99
Left precuneus (lPCUN)	Splenium of the corpus callosum (SCC)	2	−32	8	66	12.03

that were originally processed in the right hemisphere (Joseph, 1988). The rightwards functional lateralization of spatial perception was observed to be significantly increased (Cattaneoet al., 2008; Rinaldi et al., 2020). Moreover, previous studies have revealed that the right hemisphere of blind individuals is involved in tactile processing and braille reading (Gizewski et al., 2004; Jiao et al., 2023). Therefore, the enhanced original functions and the newly recruited functions in the right hemisphere maintained the E_{loc} of the right hemisphere for the CB group. However, the above interpretations of cognitive function for the different pattern of E_{loc} changes in two hemispheres are inferences based on previous studies. The relationship between structural asymmetry and functional lateralization should be revealed and discussed in further studies.

However, there was no significant difference in E_g between congenitally blind and sighted individuals. In the brain network, E_g signifies the coordination and integration between different regions, allowing information to quickly spread throughout the entire brain network (Caccetta, 1979; Ek et al., 2015; Latora and Marchiori, 2001). For individuals with congenital blindness, despite a significant decrease in the E_{loc} of the left hemisphere, the overall E_g of the brain network remained unchanged. These findings suggested that the brain maintained the overall efficiency of information transmission through compensatory mechanisms by recruiting "visual" regions to participate in other cognitive functions [i.e., auditory and tactile perception (Burton et al., 2004; Collignon et al., 2011; Dormal et al., 2016; Hötting and Röder, 2009), language processing (Amedi et al., 2004; Bedny et al., 2011; Striem-Amit et al., 2012; Watkins et al., 2012), braille reading (Burton et al., 2012; Jiao et al., 2023; Sadato et al., 1996), and mathematics (Kanjlia et al., 2016)].

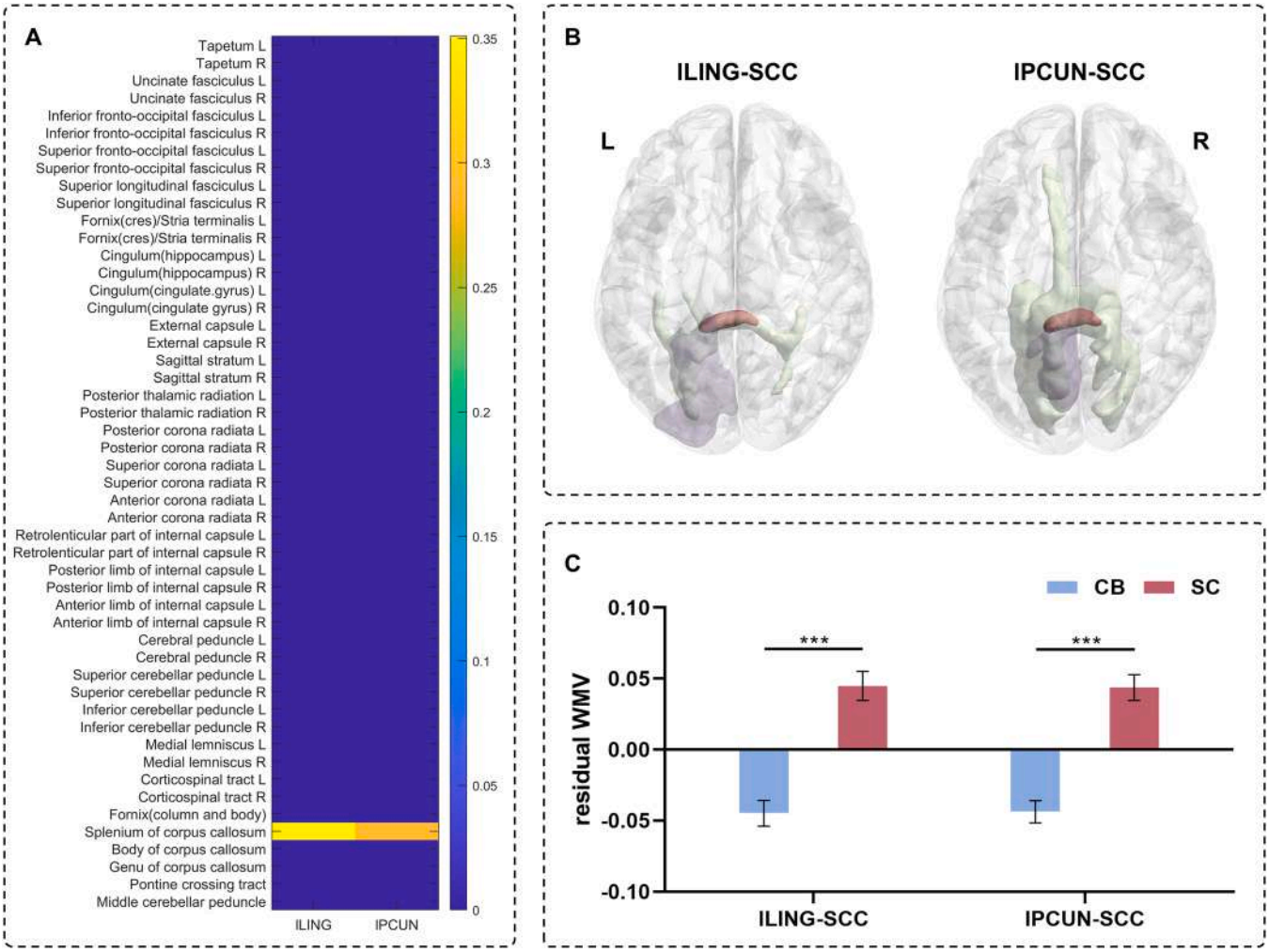

Fig. 6. The interhemispheric white matter tracts connecting the key nodes involved in asymmetry. (A) The overlap index between the interhemispheric white matter connections and the ICBM-DTI-81 atlas. (B) The lLING and lPCUN are shown in purple, and the interhemispheric white matter connections passing through the lLING and lPCUN are shown in green. The tracts with significant group differences (i.e., lLING-SCC and lPCUN-SCC) are shown in red. (C) The results of post hoc analysis for residual WMVs of the interhemispheric white matter tracts with significant group differences [i.e., the red regions in (B)] after controlling for sex and total intracranial volume. Error bars indicate the standard error of the mean. *FDR* corrected ($q < 0.001$): $^{***}P < 0.001$. CB, congenital blindness; ICBM-DTI-81, the International Consortium of Brain Mapping DTI-based atlas obtained from 81 normal subjects; l/L, left hemisphere; LING, lingual gyrus; PCUN, precuneus; R, right hemisphere; SC, sighted control; SCC, splenium of corpus callosum; WMV, white matter volume.

Overall, the brain network can undergo reorganization in response to the absence of visual input, adapting to alternative sensory inputs or enhancing nonvisual functions (Chelaru et al., 2016; De Borst and De Gelder, 2019; Gilbert and Wiesel, 1992; Keck et al., 2011; Kujala et al., 2000, 1997). This reorganization might be attributed to differences in learning experiences, environmental changes, or other factors unique to blind individuals compared to sighted individuals.The current study provided a unique insight of plastic reorganization at network-level, especially for the topological properties and asymmetries of structural network after visual loss. The structural hemispheric asymmetries may have potential as biomarkers for blind individuals.

4.2. Key brain regions related to plastic reorganization in hemispheric WM network asymmetry

$E_{loc\text{-}nodal}$ is the reciprocal of the average shortest path length between the node and its immediate neighboring nodes; E_{loc} is calculated as the average of the $E_{loc\text{-}nodal}$ of all nodes within the network (Latora and Marchiori, 2001). These two metrics exhibit a positive correlation and collectively represent the information transmission efficiency within the local subgraph (Latora and Marchiori, 2001). In the current study, we found that a reduction in the E_{loc} of the left hemisphere caused plastic reorganization of asymmetry in the hemispheric WM network in the CB group. The decrease in E_{loc} in the left hemisphere was due to “damage” to key nodes within the left hemisphere. Node-level statistical analysis revealed group alterations in the $E_{loc\text{-}nodal}$ of six key left brain regions and in the connectivity strength of their intrahemispheric connections. Almost all identified key nodes exhibited a significant reduction in blind patients compared to sighted patients, suggesting a diminished efficiency in information transmission (Latora and Marchiori, 2001) for these critical nodes and their intrahemispheric connections in the congenitally blind cohort.

These six key brain regions were distributed in the frontal lobe (i.e., lMFGorb), occipital lobe (i.e., lLING, lIOG, lPCUN, and lCUN) and subcortical areas (i.e., lPUT). Previous studies have revealed structural changes in these key regions (Voss et al., 2014). In sighted individuals, these areas are typically involved in functions such as visual processing (Bogousslavsky et al., 1987; Moores et al., 2003), spatial cognition (Horvath et al., 2019; Mahayana et al., 2014; Zündorf et al., 2013), attention (Hahn et al., 2006; Lux et al., 2003), and high-level cognitive functions that rely on visual information (e.g., language and mathematics) (Chen et al., 2020; Liu et al., 2019; Turken and Dronkers, 2011; Xu et al., 2016).

The decreased $E_{loc\text{-}nodal}$ reflected a weakening of information transmission in the local subnetworks of these functional areas, possibly related to sensory substitution and functional specificity in individuals with congenital blindness attempting to compensate for structural and functional changes caused by visual loss (Chebat et al., 2020; Collignon et al., 2006; Ptito et al., 2021). However, whether the reduction in $E_{loc\text{-}nodal}$ of these key brain regions was related to specific behaviors and cognitive functions requires further empirical evidence and research, including the use of other neuroimaging techniques (such as functional magnetic resonance imaging or electroencephalography) to validate the relationship between the changes in these brain regions and the performance of behavioral and cognitive tasks to investigate whether these changes are related to specific functions. This research will contribute to a more comprehensive understanding of the complex adaptability and structural changes in the brain networks of individuals with congenital blindness.

In conclusion, the decrease in nodal-level properties of these key brain regions provided direct evidence of neural plasticity, indicating that the brains of individuals with congenital blindness adapt to visual loss not only at the overall network level but also through structural changes in specific brain regions and their intrahemispheric connections. This finding prompted our subsequent analysis, which explored the structural reorganization of interhemispheric connections passing through the identified key brain regions.

4.3. Structural changes in the CC: physiological mechanisms of plastic reorganization in WM network asymmetry

Brain asymmetry refers to the structural and functional differences between the two hemispheres of the human brain (Duboc et al., 2015; Rentería, 2012; Toga and Thompson, 2003; Witelson, 1992, 1988). The CC serves as a bundle of WM fibers connecting the bilateral hemispheres and plays a crucial role in information transmission and coordinating activities between the two hemispheres (D. Li et al., 2021; Rosas et al., 2010; Wahl et al., 2007). Interhemispheric information exchange is crucial for ensuring the overall coordinated functioning of the brain, allowing the two hemispheres to coordinate the execution of motion, sensory perception, and complex cognitive functions (Verosky and Turk-Browne, 2012). Previous studies have shown that the structural and functional asymmetry of the brain are related to the CC (Beaton, 1997; Gilliam et al., 2011; Schutter and Harmon-Jones, 2013; Schwartz et al., 2021; Voineskos et al., 2010; Westerhausen and Hugdahl, 2008). In the more in-depth analysis, we discovered structural reorganization in the interhemispheric WM tracts connecting the "damaged" left key nodes, primarily concentrated in the SCC. The SCC, located in the posterior region, connects the bilateral occipital lobes and serves as the primary channel for information transmission in the occipital region (Berlucchi, 2014; De Lacoste et al., 1985; Degos et al., 1987). Previous research has identified structural reorganization in the SCC in blind individuals (Aguirre et al., 2016; Jiao et al., 2023; Levin et al., 2010; Ptito et al., 2008), and structural alterations were correlated with reading task performance (Jiao et al., 2023).

In this study, we not only found structural changes in the SCC but also elucidated that the structural changes in the SCC were related to WM network asymmetry. Moreover, the findings of an additional analysis for connectivity profiles between key nodes and the nodes in right hemisphere confirmed the reliable relationship between structural asymmetry and interhemispheric connections (see Supplementary Analysis 2 for further details).

Because blindness leads to the absence of visual information entering crucial occipital regions, individuals with congenital blindness exhibited a decrease in the nodal local efficiency of the occipital lobe key nodes, resulting in changes in brain asymmetry accompanied by structural changes in the SCC. The current study provides the first evidence of the relationship between brain asymmetry and the CC in individuals with congenital blindness, indicating that structural reorganization of the CC in individuals with congenital blindness might be the physiological mechanism underlying changes in asymmetry. This also enriched the understanding of the important role of the CC in maintaining efficient working of brain networks.

4.4. Limitations

The following limitations of this study should be noted. First, the current study faced limitations due to the relatively small sample size recruited, which is attributed to the rarity of individuals with congenital blindness and strict enrollment criteria. Therefore, future research efforts should focus on collecting data from a larger sample. Next, cognitive and behavioral data were not included in this study, leading to speculative discussions regarding the relationship between network asymmetry changes and language or other cognitive functions. Subsequent research should provide a more explicit assessment of the relationship between brain asymmetry and cognitive functions. Finally, this study exclusively concentrated on the plastic reorganization of WM structural network asymmetry, and corresponding investigations of functional networks to reveal the functional reorganization accompanying structural network changes were not performed.

5. Conclusion

The present study revealed the reduction of leftward asymmetry to a symmetric state in the hemispheric WM network due to a lack of congenital visual experience, which is primarily associated with "damage" to key nodes in the left hemisphere and accompanied by structural reorganization of the SCC. In-depth study of this unique topological asymmetric reorganization pattern of hemispheric WM networks provides novel insights into the neuroplasticity and adaptability of the brain, especially at the network level.

CRediT authorship contribution statement

Saiyi Jiao: Writing – review & editing, Writing – original draft, Visualization, Investigation, Formal analysis, Data curation, Conceptualization. **Ke Wang:** Investigation, Formal analysis, Data curation, Conceptualization. **Yudan Luo:** Investigation, Formal analysis, Data curation. **Jiahong Zeng:** Formal analysis, Data curation. **Zaizhu Han:** Writing – review & editing, Supervision, Investigation, Funding acquisition, Formal analysis, Conceptualization.

Declaration of competing interest

The authors declare no competing financial interests.

Data availability

Data will be made available on request.

Acknowledgement

The authors sincerely thank the members of the BNU-CN Lab for their contributions to the data collection and all participants for their time and cooperation. This work was supported by the National Natural Science Foundation of China (32271091, 81972144, 81870833, and 82372555).

Supplementary materials

Supplementary material associated with this article can be found, in the online version, at doi:10.1016/j.neuroimage.2024.120844.

References

Abboud, S., Cohen, L., 2019. Distinctive interaction between cognitive networks and the visual cortex in early blind individuals. Cereb Cortex 29, 4725–4742. https://doi.org/10.1093/cercor/bhz006.

Aboitiz, F., Scheibel, A.B., Fisher, R.S., Zaidel, E., 1992. Fiber composition of the human corpus callosum. Brain Res. 598, 143–153. https://doi.org/10.1016/0006-8993(92)90178-C.

Aguirre, G.K., Datta, R., Benson, N.C., Prasad, S., Jacobson, S.G., Cideciyan, A.V., Bridge, H., Watkins, K.E., Butt, O.H., Dain, A.S., Brandes, L., Gennatas, E.D., 2016. Patterns of individual variation in visual pathway structure and function in the sighted and blind. PLoS ONE 11, e0164677. https://doi.org/10.1371/journal.pone.0164677.

Alberto Marzi, C., 2010. Asymmetry of interhemispheric communication. WIRES Cognit. Sci. 1, 433–438. https://doi.org/10.1002/wcs.53.

Aliotti, N.C., 1981. Intelligence, handedness, and cerebral hemispheric preference in gifted adolescents. Gifted Child Q. 25, 36–41. https://doi.org/10.1177/001698628102500107.

Amedi, A., Floel, A., Knecht, S., Zohary, E., Cohen, L.G., 2004. Transcranial magnetic stimulation of the occipital pole interferes with verbal processing in blind subjects. Nat Neurosci 7, 1266–1270. https://doi.org/10.1038/nn1328.

Ashburner, J., 2007. A fast diffeomorphic image registration algorithm. Neuroimage 38, 95–113. https://doi.org/10.1016/j.neuroimage.2007.07.007.

Ashburner, J., Friston, K.J., 2000. Voxel-Based morphometry—the methods. Neuroimage 11, 805–821. https://doi.org/10.1006/nimg.2000.0582.

Barmpoutis, D., Murray, R.M., 2011. Extremal Properties of complex networks.

Barnes, J., Ridgway, G.R., Bartlett, J., Henley, S.M.D., Lehmann, M., Hobbs, N., Clarkson, M.J., MacManus, D.G., Ourselin, S., Fox, N.C., 2010. Head size, age and gender adjustment in MRI studies: a necessary nuisance? Neuroimage 53, 1244–1255. https://doi.org/10.1016/j.neuroimage.2010.06.025.

Bassett, D.S., Brown, J.A., Deshpande, V., Carlson, J.M., Grafton, S.T., 2011. Conserved and variable architecture of human white matter connectivity. Neuroimage 54, 1262–1279. https://doi.org/10.1016/j.neuroimage.2010.09.006.

Bauer, C.M., Hirsch, G.V., Zajac, L., Koo, B.-B., Collignon, O., Merabet, L.B., 2017. Multimodal MR-imaging reveals large-scale structural and functional connectivity changes in profound early blindness. PLoS ONE 12, e0173064. https://doi.org/10.1371/journal.pone.0173064.

Beaton, A.A., 1997. The relation of planum temporale asymmetry and morphology of the corpus callosum to handedness, gender, and dyslexia: a review of the evidence. Brain Lang 60, 255–322. https://doi.org/10.1006/brln.1997.1825.

Bedny, M., 2017. Evidence from blindness for a cognitively pluripotent cortex. Trends Cogn. Sci. (Regul. Ed.) 21, 637–648. https://doi.org/10.1016/j.tics.2017.06.003.

Bedny, M., Pascual-Leone, A., Dodell-Feder, D., Fedorenko, E., Saxe, R., 2011. Language processing in the occipital cortex of congenitally blind adults. Proc. Natl. Acad. Sci. U.S.A. 108, 4429–4434. https://doi.org/10.1073/pnas.1014818108.

Berlucchi, G., 2014. Visual interhemispheric communication and callosal connections of the occipital lobes. Cortex 56, 1–13. https://doi.org/10.1016/j.cortex.2013.02.001.

Binder, J.R., Frost, J.A., Hammeke, T.A., Cox, R.W., Rao, S.M., Prieto, T., 1997. Human brain language areas identified by functional magnetic resonance imaging. J. Neurosci. 17, 353–362. https://doi.org/10.1523/JNEUROSCI.17-01-00353.1997.

Bloom, J.S., Hynd, G.W., 2005. The role of the corpus callosum in interhemispheric transfer of information: excitation or inhibition? Neuropsychol. Rev. 15, 59–71. https://doi.org/10.1007/s11065-005-6252-y.

Bogousslavsky, J., Miklossy, J., Deruaz, J.P., Assal, G., Regli, F., 1987. Lingual and fusiform gyri in visual processing: a clinico-pathologic study of superior altitudinal hemianopia. J. Neurol. Neurosur. Psyc. 50, 607–614. https://doi.org/10.1136/jnnp.50.5.607.

Bosnar-Puretic, M., Roje-Bedekovic, M., Demarin, V., 2009. The art: neuroscientific approach. Acta Clin. Croat. 48.

Bullmore, E., Sporns, O., 2009. Complex brain networks: graph theoretical analysis of structural and functional systems. Nat. Rev. Neurosci. 10, 186–198. https://doi.org/10.1038/nrn2575.

Burton, H., Sinclair, R.J., Agato, A., 2012. Recognition memory for Braille or spoken words: an fMRI study in early blind. Brain Res. 1438, 22–34. https://doi.org/10.1016/j.brainres.2011.12.032.

Burton, H., Sinclair, R.J., McLaren, D.G., 2004. Cortical activity to vibrotactile stimulation: an fMRI study in blind and sighted individuals. Hum. Brain Mapp. 23, 210–228. https://doi.org/10.1002/hbm.20064.

Caccetta, L., 1979. ON EXTREMAL GRAPHS WITH GIVEN DIAMETER AND CONNECTIVITY. Ann. N. Y. Acad. Sci. 328, 76–94. https://doi.org/10.1111/j.1749-6632.1979.tb17769.x.

Caeyenberghs, K., Leemans, A., 2014. Hemispheric lateralization of topological organization in structural brain networks. Hum. Brain Mapp 35, 4944–4957. https://doi.org/10.1002/hbm.22524.

Cai, L., Dong, Q., Wang, M., Niu, H., 2019. Functional near-infrared spectroscopy evidence for the development of topological asymmetry between hemispheric brain networks from childhood to adulthood. Neurophotonics 6, 025005. https://doi.org/10.1117/1.NPh.6.2.025005.

Carota, A., Bogousslavsky, Julien, 2018. Minor hemisphere major syndromes. In: Bogousslavsky, J. (Ed.), Minor hemisphere major syndromes. Front. Neurol. Neurosci. 1–13. https://doi.org/10.1159/000475690. S. Karger AG.

Cattaneo, Z., Vecchi, T., Cornoldi, C., Mammarella, I., Bonino, D., Ricciardi, E., Pietrini, P., 2008. Imagery and spatial processes in blindness and visual impairment. Neurosci. Biobehav. Rev. 32, 1346–1360. https://doi.org/10.1016/j.neubiorev.2008.05.002.

Cavaliere, C., Aiello, M., Soddu, A., Laureys, S., Reislev, N.L., Ptito, M., Kupers, R., 2020. Organization of the commissural fiber system in congenital and late-onset blindness. NeuroImage Clin. 25, 102133 https://doi.org/10.1016/j.nicl.2019.102133.

Celeghin, A., Diano, M., De Gelder, B., Weiskrantz, L., Marzi, C.A., Tamietto, M., 2017. Intact hemisphere and corpus callosum compensate for visuomotor functions after early visual cortex damage. Proc. Natl. Acad. Sci. U.S.A. 114 https://doi.org/10.1073/pnas.1714801114.

Chebat, D.-R., Schneider, F.C., Ptito, M., 2020. Spatial competence and brain plasticity in congenital blindness via sensory substitution devices. Front. Neurosci. 14, 815. https://doi.org/10.3389/fnins.2020.00815.

Chelaru, M.I., Hansen, B.J., Tandon, N., Conner, C.R., Szukalski, S., Slater, J.D., Kalamangalam, G.P., Dragoi, V., 2016. Reactivation of visual-evoked activity in human cortical networks. J. Neurophysiol. 115, 3090–3100. https://doi.org/10.1152/jn.00724.2015.

Chen, Y., Huang, L., Chen, K., Ding, J., Zhang, Y., Yang, Q., Lv, Y., Han, Z., Guo, Q., 2020. White matter basis for the hub-and-spoke semantic representation: evidence from semantic dementia. Brain 143, 1206–1219. https://doi.org/10.1093/brain/awaa057.

Chiarello, C., Vazquez, D., Felton, A., Leonard, C.M., 2013. Structural asymmetry of anterior insula: behavioral correlates and individual differences. Brain Lang 126, 109–122. https://doi.org/10.1016/j.bandl.2013.03.005.

Collignon, O., Davare, M., Olivier, E., De Volder, A.G., 2009. Reorganisation of the right occipito-parietal stream for auditory spatial processing in early blind humans. a transcranial magnetic stimulation study. Brain Topogr. 21, 232–240. https://doi.org/10.1007/s10548-009-0075-8.

Collignon, O., Lassonde, M., Lepore, F., Bastien, D., Veraart, C., 2006. Functional cerebral reorganization for auditory spatial processing and auditory substitution of vision in early blind subjects. Cerebral Cortex 17, 457–465. https://doi.org/10.1093/cercor/bhj162.

Collignon, O., Vandewalle, G., Voss, P., Albouy, G., Charbonneau, G., Lassonde, M., Lepore, F., 2011. Functional specialization for auditory–spatial processing in the occipital cortex of congenitally blind humans. Proc. Natl. Acad. Sci. U.S.A. 108, 4435–4440. https://doi.org/10.1073/pnas.1013928108.

Cona, G., Scarpazza, C., 2019. Where is the "where" in the brain? A meta-analysis of neuroimaging studies on spatial cognition. Hum. Brain Mapp. 40, 1867–1886. https://doi.org/10.1002/hbm.24496.

Cui, Z., Zhong, S., Xu, P., He, Y., Gong, G., 2013. PANDA: a pipeline toolbox for analyzing brain diffusion images. Front. Hum. Neurosci. 7 https://doi.org/10.3389/fnhum.2013.00042.

De Borst, A.W., De Gelder, B., 2019. Mental imagery follows similar cortical reorganization as perception: intra-modal and cross-modal plasticity in congenitally blind. Cerebral Cortex 29, 2859–2875. https://doi.org/10.1093/cercor/bhy151.

De Lacoste, M.C., Kirkpatrick, J.B., Ross, E.D., 1985. Topography of the human corpus callosum. J. Neuropathol. Exp. Neurol. 44, 578–591. https://doi.org/10.1097/00005072-198511000-00004.

Degos, J.D., Gray, F., Louarn, F., Ansquer, J.C., Poirier, J., Barbizet, J., 1987. Posterior callosal infarction: clinicopathological correlations. Brain 110, 1155–1171. https://doi.org/10.1093/brain/110.5.1155.

Dennis, E.L., Jahanshad, N., McMahon, K.L., De Zubicaray, G.I., Martin, N.G., Hickie, I. B., Toga, A.W., Wright, M.J., Thompson, P.M., 2013. Development of brain structural connectivity between ages 12 and 30: a 4-Tesla diffusion imaging study in 439 adolescents and adults. Neuroimage 64, 671–684. https://doi.org/10.1016/j.neuroimage.2012.09.004.

Di Ciò, F., Garaci, F., Minosse, S., Passamonti, L., Martucci, A., Lanzafame, S., Di Giuliano, F., Picchi, E., Cesareo, M., Guerrisi, M.G., Floris, R., Nucci, C., Toschi, N., 2020. Reorganization of the structural connectome in primary open angle Glaucoma. Neuroimage Clin. 28, 102419 https://doi.org/10.1016/j.nicl.2020.102419.

Dormal, G., Rezk, M., Yakobov, E., Lepore, F., Collignon, O., 2016. Auditory motion in the sighted and blind: early visual deprivation triggers a large-scale imbalance between auditory and "visual" brain regions. Neuroimage 134, 630–644. https://doi.org/10.1016/j.neuroimage.2016.04.027.

Duboc, V., Dufourcq, P., Blader, P., Roussigné, M., 2015. Asymmetry of the Brain: development and Implications. Annu. Rev. Genet. 49, 647–672. https://doi.org/10.1146/annurev-genet-112414-055322.

Duda, J.T., Cook, P.A., Gee, J.C., 2014. Reproducibility of graph metrics of human brain structural networks. Front. Neuroinf.. 8 https://doi.org/10.3389/fninf.2014.00046.

Ek, B., VerSchneider, C., Narayan, D.A., 2015. Global efficiency of graphs. AKCE Int. J. Graphs Combinator. 12, 1–13. https://doi.org/10.1016/j.akcej.2015.06.001.

Esteves, M., Lopes, S.S., Almeida, A., Sousa, N., Leite-Almeida, H., 2020. Unmasking the relevance of hemispheric asymmetries—Break on through (to the other side). Prog. Neurobiol. 192, 101823 https://doi.org/10.1016/j.pneurobio.2020.101823.

Fitch, W.T., Braccini, S.N., 2013. Primate laterality and the biology and evolution of human handedness: a review and synthesis. Ann. N. Y. Acad. Sci. 1288, 70–85. https://doi.org/10.1111/nyas.12071.

Genovese, C.R., Lazar, N.A., Nichols, T., 2002. Thresholding of statistical maps in functional neuroimaging using the false discovery rate. Neuroimage 15, 870–878. https://doi.org/10.1006/nimg.2001.1037.

Gilbert, C.D., Wiesel, T.N., 1992. Receptive field dynamics in adult primary visual cortex. Nature 356, 150–152. https://doi.org/10.1038/356150a0.

Gilliam, M., Stockman, M., Malek, M., Sharp, W., Greenstein, D., Lalonde, F., Clasen, L., Giedd, J., Rapoport, J., Shaw, P., 2011. Developmental trajectories of the corpus callosum in attention-deficit/hyperactivity disorder. Biol. Psychiatry 69, 839–846. https://doi.org/10.1016/j.biopsych.2010.11.024.

Gizewski, E.R., Timmann, D., Forsting, M., 2004. Specific cerebellar activation during Braille reading in blind subjects. Hum. Brain Mapp. 22, 229–235. https://doi.org/10.1002/hbm.20031.

Goldszal, A.F., Davatzikos, C., Pham, D.L., Yan, M.X.H., Bryan, R.N., Resnick, S.M., 1998. An image-processing system for qualitative and quantitative volumetric analysis of brain images. J.Comput. Assisted Tomogr. 22, 827–837. https://doi.org/10.1097/00004728-199809000-00030.

Gong, G., He, Y., Concha, L., Lebel, C., Gross, D.W., Evans, A.C., Beaulieu, C., 2009a. Mapping anatomical connectivity patterns of human cerebral cortex using in vivo diffusion tensor imaging tractography. Cerebral Cortex 19, 524–536. https://doi.org/10.1093/cercor/bhn102.

Gong, G., Rosa-Neto, P., Carbonell, F., Chen, Z.J., He, Y., Evans, A.C., 2009b. Age- and gender-related differences in the cortical anatomical network. J. Neurosci. 29, 15684–15693. https://doi.org/10.1523/JNEUROSCI.2308-09.2009.

Greenough, W.T., Black, J.E., Wallace, C.S., 1987. Experience and brain development. Child Dev 58, 539. https://doi.org/10.2307/1130197.

Hahn, B., Ross, T.J., Stein, E.A., 2006. Neuroanatomical dissociation between bottom–up and top–down processes of visuospatial selective attention. Neuroimage 32, 842–853. https://doi.org/10.1016/j.neuroimage.2006.04.177.

Hamilton, R.H., Pascual-Leone, A., Schlaug, G., 2004. Absolute pitch in blind musicians. Neuroreport 15, 803–806. https://doi.org/10.1097/00001756-200404090-00012.

Horvath, A., Kiss, M., Szucs, A., Kamondi, A., 2019. Precuneus-dominant degeneration of parietal lobe is at risk of epilepsy in mild Alzheimer's disease. Front. Neurol. 10, 878. https://doi.org/10.3389/fneur.2019.00878.

Hötting, K., Röder, B., 2009. Auditory and auditory-tactile processing in congenitally blind humans. Hear. Res. 258, 165–174. https://doi.org/10.1016/j.heares.2009.07.012.

Jiao, S., Wang, K., Zhang, L., Luo, Y., Lin, J., Han, Z., 2023. Developmental plasticity of the structural network of the occipital cortex in congenital blindness. Cerebral Cortex 33, 11526–11540. https://doi.org/10.1093/cercor/bhad385.

Joseph, R., 1988. The right cerebral hemisphere: emotion, music, visual-spatial skills, body-image, dreams, and awareness. J. Clin. Psychol. 44, 630–673. https://doi.org/10.1002/1097-4679(198809)44:5<630::AID-JCLP2270440502>3.0.CO;2-V.

Kanjlia, S., Lane, C., Feigenson, L., Bedny, M., 2016. Absence of visual experience modifies the neural basis of numerical thinking. Proc. Natl. Acad. Sci. U.S.A. 113, 11172–11177. https://doi.org/10.1073/pnas.1524982113.

Keck, T., Scheuss, V., Jacobsen, R.I., Wierenga, C.J., Eysel, U.T., Bonhoeffer, T., Hübener, M., 2011. Loss of sensory input causes rapid structural changes of inhibitory neurons in adult mouse visual cortex. Neuron 71, 869–882. https://doi.org/10.1016/j.neuron.2011.06.034.

Kim, J.S., Kanjlia, S., Merabet, L.B., Bedny, M., 2017. Development of the visual word form area requires visual experience: evidence from blind braille readers. J. Neurosci. 37, 11495–11504. https://doi.org/10.1523/JNEUROSCI.0997-17.2017.

Knijnenburg, T.A., Wessels, L.F.A., Reinders, M.J.T., Shmulevich, I., 2009. Fewer permutations, more accurate *P* -values. Bioinformatics 25, i161–i168. https://doi.org/10.1093/bioinformatics/btp211.

Koelsch, S., Fritz, T., Schulze, K., Alsop, D., Schlaug, G., 2005. Adults and children processing music: an fMRI study. Neuroimage 25, 1068–1076. https://doi.org/10.1016/j.neuroimage.2004.12.050.

Kolb, B., 1998. Age, experience and the changing brain. Neurosci. Biobehav. Rev. 22, 143–159. https://doi.org/10.1016/S0149-7634(97)00008-0.

Kujala, T., Alho, K., Huotilainen, M., Ilmoniemi, R.J., Lehtokoski, A., Leinonen, A., Rinne, T., Salonen, O., Sinkkonen, J., Standertskjöuld-Nordenstam, C.-G., Näuäutäunen, R., 1997. Electrophysiological evidence for cross-modal plasticity in humans with early- and late-onset blindness. Psychophysiology 34, 213–216. https://doi.org/10.1111/j.1469-8986.1997.tb02134.x.

Kujala, T., Alho, K., Näätänen, R., 2000. Cross-modal reorganization of human cortical functions. Trends Neurosci. 23, 115–120. https://doi.org/10.1016/S0166-2236(99)01504-0.

Labache, L., Mazoyer, B., Joliot, M., Crivello, F., Hesling, I., Tzourio-Mazoyer, N., 2020. Typical and atypical language brain organization based on intrinsic connectivity and multitask functional asymmetries. eLife 9, e58722. https://doi.org/10.7554/eLife.58722.

Lane, C., Kanjlia, S., Richardson, H., Fulton, A., Omaki, A., Bedny, M., 2017. Reduced left lateralization of language in congenitally blind individuals. J. Cogn. Neurosci. 29, 65–78. https://doi.org/10.1162/jocn_a_01045.

Latora, V., Marchiori, M., 2001. Efficient behavior of small-world networks. Phys. Rev. Lett. 87, 198701 https://doi.org/10.1103/PhysRevLett.87.198701.

Leemans, A., Jones, D.K., 2009. The *B* -matrix must be rotated when correcting for subject motion in DTI data. Magnet. Resonance Med. 61, 1336–1349. https://doi.org/10.1002/mrm.21890.

Leporé, N., Voss, P., Lepore, F., Chou, Y.-Y., Fortin, M., Gougoux, F., Lee, A.D., Brun, C., Lassonde, M., Madsen, S.K., Toga, A.W., Thompson, P.M., 2010. Brain structure changes visualized in early- and late-onset blind subjects. Neuroimage 49, 134–140. https://doi.org/10.1016/j.neuroimage.2009.07.048.

Levin, N., Dumoulin, S.O., Winawer, J., Dougherty, R.F., Wandell, B.A., 2010. Cortical maps and white matter tracts following long period of visual deprivation and retinal image restoration. Neuron 65, 21–31. https://doi.org/10.1016/j.neuron.2009.12.006.

Li, D., Tang, W., Yan, T., Zhang, N., Xiang, J., Niu, Y., Wang, B., 2021a. Abnormalities in hemispheric lateralization of intra- and inter-hemispheric white matter connections in schizophrenia. Brain Imaging Behav. 15, 819–832. https://doi.org/10.1007/s11682-020-00292-9.

Li, J., Liu, Y., Qin, W., Jiang, J., Qiu, Z., Xu, J., Yu, C., Jiang, T., 2013. Age of onset of blindness affects brain anatomical networks constructed using diffusion tensor tractography. Cerebral Cortex 23, 542–551. https://doi.org/10.1093/cercor/bhs034.

Li, M., Liu, T., Xu, X., Wen, Q., Zhao, Z., Dang, X., Zhang, Y., Wu, D., 2022. Development of visual cortex in human neonates is selectively modified by postnatal experience. Elife 11, e78733. https://doi.org/10.7554/eLife.78733.

Li, M., Song, L., Zhang, Y., Han, Z., 2021. White matter network of oral word reading identified by network-based lesion-symptom mapping. iScience 24, 102862. 10.1016/j.isci.2021.102862.

Li, Y., Liu, Y., Li, J., Qin, W., Li, K., Yu, C., Jiang, T., 2009. Brain anatomical network and intelligence. PLoS Comput. Biol. 5.

Lin, J., Zhang, L., Guo, R., Jiao, S., Song, X., Feng, S., Wang, K., Li, M., Luo, Y., Han, Z., 2022. The influence of visual deprivation on the development of the thalamocortical network: evidence from congenitally blind children and adults. Neuroimage 264, 119722. https://doi.org/10.1016/j.neuroimage.2022.119722.

Liu, J., Yuan, L., Chen, C., Cui, J., Zhang, H., Zhou, X., 2019. The semantic system supports the processing of mathematical principles. Neuroscience 404, 102–118. https://doi.org/10.1016/j.neuroscience.2019.01.043.

López-Bendito, G., Aníbal-Martínez, M., Martini, F.J., 2022. Cross-modal plasticity in brains deprived of visual input before vision. Annu. Rev. Neurosci. 45, 471–489. https://doi.org/10.1146/annurev-neuro-111020-104222.

Lux, S., Marshall, J.C., Ritzl, A., Zilles, K., Fink, G.R., 2003. Neural mechanisms associated with attention to temporal synchrony versus spatial orientation: an fMRI study. Neuroimage 20, S58–S65. https://doi.org/10.1016/j.neuroimage.2003.09.009.

Mahayana, I.T., Tcheang, L., Chen, C.-Y., Juan, C.-H., Muggleton, N.G., 2014. The precuneus and visuospatial attention in near and far space: a transcranial magnetic stimulation study. Brain Stimul 7, 673–679. https://doi.org/10.1016/j.brs.2014.06.012.

Moores, K.A., Clark, C.R., Hadfield, J.L.M., Brown, G.C., Taylor, D.J., Fitzgibbon, S.P., Lewis, A.C., Weber, D.L., Greenblatt, R., 2003. Investigating the generators of the

scalp recorded visuo-verbal P300 using cortically constrained source localization. Hum. Brain Mapp 18, 53–77. https://doi.org/10.1002/hbm.10073.
Mori, S., Crain, B.J., Chacko, V.P., Van Zijl, P.C.M., 1999. Three-dimensional tracking of axonal projections in the brain by magnetic resonance imaging. Ann. Neurol. 45, 265–269. https://doi.org/10.1002/1531-8249(199902)45:2<265::AID-ANA21>3.0.CO;2-3.
Mori, S., Oishi, K., Jiang, H., Jiang, L., Li, X., Akhter, K., Hua, K., Faria, A.V., Mahmood, A., Woods, R., Toga, A.W., Pike, G.B., Neto, P.R., Evans, A., Zhang, J., Huang, H., Miller, M.I., Van Zijl, P., Mazziotta, J., 2008. Stereotaxic white matter atlas based on diffusion tensor imaging in an ICBM template. Neuroimage 40, 570–582. https://doi.org/10.1016/j.neuroimage.2007.12.035.
Mori, S., van Zijl, P.C.M., 2002. Fiber tracking: principles and strategies - a technical review. NMR Biomed 15, 468–480. https://doi.org/10.1002/nbm.781.
Nikolaenko, N.N., 1998. Interaction of Cerebral Hemispheres and Artistic Thinking, in: Rogowitz, B.E., Pappas, T.N.. Presented at the Photonics West '98 Electronic Imaging, San Jose, CA, pp. 439–446. 10.1117/12.320134.
Nucifora, P.G.P., Verma, R., Melhem, E.R., Gur, R.E., Gur, R.C., 2005. Leftward asymmetry in relative fiber density of the arcuate fasciculus. Neuroreport 16, 791.
Oldfield, R.C., 1971. The assessment and analysis of handedness: the Edinburgh inventory. Neuropsychologia 9, 97–113. https://doi.org/10.1016/0028-3932(71)90067-4.
Pan, W.-J., Wu, G.-Y., Li, C., Lin, F.-C., Sun, J.-M., Lei, H., 2008. Gray matter asymmetry of early blind human: a voxel-based mophometry study. Chinese J. Med. Imaging Technology 24, 333–335.
Park, H.-J., Friston, K., 2013. Structural and functional brain networks: from connections to cognition. Science 342, 1238411. https://doi.org/10.1126/science.1238411.
Ptito, M., Bleau, M., Djerourou, I., Paré, S., Schneider, F.C., Chebat, D.-R., 2021. Brain-machine interfaces to assist the blind. Front. Hum. Neurosci. 15, 638887 https://doi.org/10.3389/fnhum.2021.638887.
Ptito, M., Schneider, F.C.G., Paulson, O.B., Kupers, R., 2008. Alterations of the visual pathways in congenital blindness. Exp. Brain Res. 187, 41–49. https://doi.org/10.1007/s00221-008-1273-4.
Qiu, D., Tan, L., Siok, W., Zhou, K., Khong, P., 2011. Lateralization of the arcuate fasciculus and its differential correlation with reading ability between young learners and experienced readers: a diffusion tensor tractography study in a chinese cohort. Hum. Brain Mapp. 32, 2054–2063. https://doi.org/10.1002/hbm.21168.
Ratnarajah, N., Rifkin-Graboi, A., Fortier, M.V., Chong, Y.S., Kwek, K., Saw, S.-M., Godfrey, K.M., Gluckman, P.D., Meaney, M.J., Qiu, A., 2013. Structural connectivity asymmetry in the neonatal brain. Neuroimage 75, 187–194. https://doi.org/10.1016/j.neuroimage.2013.02.052.
Rentería, M.E., 2012. Cerebral asymmetry: a quantitative, multifactorial, and plastic brain phenotype. Twin Res. Hum Genet. 15, 401–413. https://doi.org/10.1017/thg.2012.13.
Rinaldi, L., Ciricugno, A., Merabet, L.B., Vecchi, T., Cattaneo, Z., 2020. The effect of blindness on spatial asymmetries. Brain Sci 10, 662. https://doi.org/10.3390/brainsci10100662.
Rosas, H.D., Lee, S.Y., Bender, A.C., Zaleta, A.K., Vangel, M., Yu, P., Fischl, B., Pappu, V., Onorato, C., Cha, J.-H., Salat, D.H., Hersch, S.M., 2010. Altered white matter microstructure in the corpus callosum in Huntington's disease: implications for cortical "disconnection. Neuroimage 49, 2995–3004. https://doi.org/10.1016/j.neuroimage.2009.10.015.
Sadato, N., Pascual-Leone, A., Grafman, J., Ibañez, V., Deiber, M.-P., Dold, G., Hallett, M., 1996. Activation of the primary visual cortex by Braille reading in blind subjects. Nature 380, 526–528. https://doi.org/10.1038/380526a0.
Schutter, D.J.L.G., Harmon-Jones, E., 2013. The corpus callosum: a commissural road to anger and aggression. Neuroscie. Biobehav. Rev. 37, 2481–2488. https://doi.org/10.1016/j.neubiorev.2013.07.013.
IRC5 consortium Schwartz, E., Diogo, M.C., Glatter, S., Seidl, R., Brugger, P.C., Gruber, G.M., Kiss, H., Nenning, K.-H., Langs, G., Prayer, D., Kasprian, G., 2021. The prenatal morphomechanic impact of agenesis of the corpus callosum on human brain structure and asymmetry. Cerebral Cortex, bhab066. https://doi.org/10.1093/cercor/bhab066.
Shi, J., Collignon, O., Xu, L., Wang, G., Kang, Y., Leporé, F., Lao, Y., Joshi, A.A., Leporé, N., Wang, Y., 2015. Impact of early and late visual deprivation on the structure of the corpus callosum: a study combining thickness profile with surface tensor-based morphometry. Neuroinform 13, 321–336. https://doi.org/10.1007/s12021-014-9259-9.
Shu, N., Li, J., Li, K., Yu, C., Jiang, T., 2009a. Abnormal diffusion of cerebral white matter in early blindness. Hum Brain Mapp 30, 220–227. https://doi.org/10.1002/hbm.20507.
Shu, N., Liu, Y., Li, J., Li, Y., Yu, C., Jiang, T., 2009b. Altered anatomical network in early blindness revealed by diffusion tensor tractography. PLoS ONE 4, e7228. https://doi.org/10.1371/journal.pone.0007228.
Shu, N., Liu, Y., Li, K., Duan, Y., Wang, J., Yu, C., Dong, H., Ye, J., He, Y., 2011. Diffusion tensor tractography reveals disrupted topological efficiency in white matter structural networks in multiple sclerosis. Cerebral Cortex 21, 2565–2577. https://doi.org/10.1093/cercor/bhr039.
Spillane, J.D., 1960. The corpus callosum. Brain 83, 351. https://doi.org/10.1093/brain/83.2.351.
Sporns, O., 2018. Graph theory methods: applications in brain networks. Dialogues Clin Neurosci 20, 111–121. https://doi.org/10.31887/DCNS.2018.20.2/osporns.
Sporns, O., 2013. Structure and function of complex brain networks. Dialogues Clin Neurosci 15, 247–262. https://doi.org/10.31887/DCNS.2013.15.3/osporns.
Striem-Amit, E., Cohen, L., Dehaene, S., Amedi, A., 2012. Reading with sounds: sensory substitution selectively activates the visual word form area in the blind. Neuron 76, 640–652. https://doi.org/10.1016/j.neuron.2012.08.026.
Sun, Y., Chen, Y., Collinson, S.L., Bezerianos, A., Sim, K., 2017. Reduced hemispheric asymmetry of brain anatomical networks is linked to schizophrenia: a connectome study. Cerebral Cortex 27, 602–615. https://doi.org/10.1093/cercor/bhv255.
Szczupak, D., Iack, P.M., Rayée, D., Liu, C., Lent, R., Tovar-Moll, F., Silva, A.C., 2023. The relevance of heterotopic callosal fibers to interhemispheric connectivity of the mammalian brain. Cerebral Cortex 33, 4752–4760. https://doi.org/10.1093/cercor/bhac377.
Theofanopoulou, C., 2015. Brain asymmetry in the white matter making and globularity. Front. Psychol. 6 https://doi.org/10.3389/fpsyg.2015.01355.
Tian, S., Chen, L., Wang, Xiaoying, Li, G., Fu, Z., Ji, Y., Lu, J., Wang, Xiaosha, Shan, S., Bi, Y., 2024. Vision matters for shape representation: evidence from sculpturing and drawing in the blind. Cortex 174, 241–255. https://doi.org/10.1016/j.cortex.2024.02.016.
Toga, A.W., Thompson, P.M., 2003. Mapping brain asymmetry. Nat Rev Neurosci 4, 37–48. https://doi.org/10.1038/nrn1009.
Tomaiuolo, F., Campana, S., Collins, D.L., Fonov, V.S., Ricciardi, E., Sartori, G., Pietrini, P., Kupers, R., Ptito, M., 2014. Morphometric changes of the corpus callosum in congenital blindness. PLoS ONE 9, e107871. https://doi.org/10.1371/journal.pone.0107871.
Turken, A.U., Dronkers, N.F., 2011. The Neural architecture of the language comprehension network: converging evidence from lesion and connectivity analyses. Front. Syst. Neurosci. 5 https://doi.org/10.3389/fnsys.2011.00001.
Tzourio-Mazoyer, N., Landeau, B., Papathanassiou, D., Crivello, F., Etard, O., Delcroix, N., Mazoyer, B., Joliot, M., 2002. Automated anatomical labeling of activations in SPM Using a macroscopic anatomical parcellation of the MNI MRI single-subject brain. Neuroimage 15, 273–289. https://doi.org/10.1006/nimg.2001.0978.
Van Den Heuvel, M.P., Sporns, O., 2011. Rich-Club organization of the human connectome. J. Neurosci. 31, 15775–15786. https://doi.org/10.1523/JNEUROSCI.3539-11.2011.
Van Mieghem, P., 2023. Graph Spectra for Complex Networks, 2nd ed. Cambridge University Press. https://doi.org/10.1017/9781009366793.
Vaquero, L., Ramos-Escobar, N., François, C., Penhune, V., Rodríguez-Fornells, A., 2018. White-matter structural connectivity predicts short-term melody and rhythm learning in non-musicians. Neuroimage 181, 252–262. https://doi.org/10.1016/j.neuroimage.2018.06.054.
Verosky, S.C., Turk-Browne, N.B., 2012. Representations of facial identity in the left hemisphere require right hemisphere processing. J. Cogn. Neurosci. 24, 1006–1017. https://doi.org/10.1162/jocn_a_00196.
Voineskos, A.N., Farzan, F., Barr, M.S., Lobaugh, N.J., Mulsant, B.H., Chen, R., Fitzgerald, P.B., Daskalakis, Z.J., 2010. The role of the corpus callosum in transcranial magnetic stimulation induced interhemispheric signal propagation. Biol. Psychiatry 68, 825–831. https://doi.org/10.1016/j.biopsych.2010.06.021.
Voss, P., Pike, B.G., Zatorre, R.J., 2014. Evidence for both compensatory plastic and disuse atrophy-related neuroanatomical changes in the blind. Brain 137, 1224–1240. https://doi.org/10.1093/brain/awu030.
Wahl, M., Lauterbach-Soon, B., Hattingen, E., Jung, P., Singer, O., Volz, S., Klein, J.C., Steinmetz, H., Ziemann, U., 2007. Human Motor Corpus Callosum: topography, Somatotopy, and Link between Microstructure and Function. J. Neurosci. 27, 12132–12138. https://doi.org/10.1523/JNEUROSCI.2320-07.2007.
Wang, J., Wang, X., Xia, M., Liao, X., Evans, A., He, Y., 2015. GRETNA: a graph theoretical network analysis toolbox for imaging connectomics. Front. Hum. Neurosci. 9 https://doi.org/10.3389/fnhum.2015.00386.
Wang, X., He, C., Peelen, M.V., Zhong, S., Gong, G., Caramazza, A., Bi, Y., 2017. Domain Selectivity in the Parahippocampal Gyrus Is Predicted by the Same Structural Connectivity Patterns in Blind and Sighted Individuals. J. Neurosci. 37, 4705–4716. https://doi.org/10.1523/JNEUROSCI.3622-16.2017.
Wang, X., Lin, Q., Xia, M., He, Y., 2018. Differentially categorized structural brain hubs are involved in different microstructural, functional, and cognitive characteristics and contribute to individual identification. Hum Brain Mapp. 39, 1647–1663. https://doi.org/10.1002/hbm.23941.
Watkins, K.E., Cowey, A., Alexander, I., Filippini, N., Kennedy, J.M., Smith, S.M., Ragge, N., Bridge, H., 2012. Language networks in anophthalmia: maintained hierarchy of processing in 'visual' cortex. Brain 135, 1566–1577. https://doi.org/10.1093/brain/aws067.
Wei, L., Zhong, S., Nie, S., Gong, G., 2018. Aberrant development of the asymmetry between hemispheric brain white matter networks in autism spectrum disorder. Eur. Neuropsychopharmacol. 28, 48–62. https://doi.org/10.1016/j.euroneuro.2017.11.018.
Westerhausen, R., Hugdahl, K., 2008. The corpus callosum in dichotic listening studies of hemispheric asymmetry: a review of clinical and experimental evidence. Neurosci. Biobehav. Rev. 32, 1044–1054. https://doi.org/10.1016/j.neubiorev.2008.04.005.
Witelson, S.F., 1992. Cognitive neuroanatomy. Neurology 42. https://doi.org/10.1212/WNL.42.4.709, 709–709.
Witelson, S.F., 1988. Brain Asymmetry, Functional Aspects, in: Hobson, J.A., States of Brain and Mind, Readings from The. Birkhäuser, Boston, MA, pp. 13–16. 10.1007/978-1-4899-6771-8_6.
Xu, S., Yao, X., Han, L., Lv, Y., Bu, X., Huang, Gan, Fan, Y., Yu, T., Huang, Gang., 2021. Brain network analyses of diffusion tensor imaging for brain aging. MBE 18, 6066–6078. https://doi.org/10.3934/mbe.2021303.
Xu, Y., Lin, Q., Han, Z., He, Y., Bi, Y., 2016. Intrinsic functional network architecture of human semantic processing: modules and hubs. Neuroimage 132, 542–555. https://doi.org/10.1016/j.neuroimage.2016.03.004.
Yan, C., Gong, G., Wang, J., Wang, D., Liu, D., Zhu, C., Chen, Z.J., Evans, A., Zang, Y., He, Y., 2011. Sex- and brain size–related small-world structural cortical networks in

young adults: a DTI tractography study. Cerebral Cortex 21, 449–458. https://doi.org/10.1093/cercor/bhq111.

Yang, C., Zhong, S., Zhou, X., Wei, L., Wang, L., Nie, S., 2017. The abnormality of topological asymmetry between hemispheric brain white matter networks in Alzheimer's disease and mild cognitive impairment. Front. Aging Neurosci. 9, 261. https://doi.org/10.3389/fnagi.2017.00261.

Zalesky, A., Fornito, A., Harding, I.H., Cocchi, L., Yücel, M., Pantelis, C., Bullmore, E.T., 2010. Whole-brain anatomical networks: does the choice of nodes matter? Neuroimage 50, 970–983. https://doi.org/10.1016/j.neuroimage.2009.12.027.

Zatorre, R.J., Bouffard, M., Ahad, P., Belin, P., 2002. Where is "where" in the human auditory cortex? Nat Neurosci 5, 905–909. https://doi.org/10.1038/nn904.

Zhang, Y., Tan, W., Jiang, C., Xu, C., Wang, L., Chen, Y., Gong, Z., Huang, Y., Wang, H., Kang, Y., 2023. Study of structural network topological properties of vascular cognitive impairment based on graph theory anlysis. Chinese Imag. J. Int. Trad. Western Med. 21, 275–278.

Zhao, C., Yang, L., Xie, S., Zhang, Z., Pan, H., Gong, G., 2019. Hemispheric module-specific influence of the X chromosome on white matter connectivity: evidence from girls with turner syndrome. Cerebral. Cortex 29, 4580–4594. https://doi.org/10.1093/cercor/bhy335.

Zhong, S., He, Y., Gong, G., 2015. Convergence and divergence across construction methods for human brain white matter networks: an assessment based on individual differences. Hum Brain Mapp 36, 1995–2013. https://doi.org/10.1002/hbm.22751.

Zhong, S., He, Y., Shu, H., Gong, G., 2016. Developmental changes in topological asymmetry between hemispheric brain white matter networks from adolescence to young adulthood. Cereb. Cortex bhw 109. https://doi.org/10.1093/cercor/bhw109.

Zhong, S., Wei, L., Zhao, C., Yang, L., Di, Z., Francks, C., Gong, G., 2021. Interhemispheric relationship of genetic influence on human brain connectivity. Cerebral Cortex 31, 77–88. https://doi.org/10.1093/cercor/bhaa207.

Zhou, Y., Wang, J., 2018. Efficiency of complex networks under failures and attacks: a percolation approach. Phys. A Stat. Mech. Appl. 512, 658–664. https://doi.org/10.1016/j.physa.2018.08.093.

Zhou, Z., Qian, L., Xu, J., Lu, Y., Hou, F., Zhou, J., Luo, J., Hou, G., Jiang, W., Li, H., Liu, X., 2022. Topologic reorganization of white matter connectivity networks in early-blind adolescents. Neural Plast. 2022, 1–11. https://doi.org/10.1155/2022/8034757.

Zhu, Y., Wang, S., Gong, X., Edmiston, E.K., Zhong, S., Li, C., Zhao, P., Wei, S., Jiang, X., Qin, Y., Kang, J., Wang, Y., Sun, Q., Gong, G., Wang, F., Tang, Y., 2021. Associations between hemispheric asymmetry and schizophrenia-related risk genes in people with schizophrenia and people at a genetic high risk of schizophrenia. Br. J. Psychiatry 219, 392–400. https://doi.org/10.1192/bjp.2021.47.

Zündorf, I.C., Lewald, J., Karnath, H.O., 2013. Neural correlates of sound localization in complex acoustic environments. PLoS ONE 8, e64259. https://doi.org/10.1371/journal.pone.0064259.